

INSIGHTS INTO THE METABOLIC REGULATION BY
GATOR1 IN RESPONSE TO AMINO ACID SIGNALING

APPROVED BY SUPERVISORY COMMITTEE

Benjamin P. Tu, Ph.D., Supervisor

Yi Liu, Ph.D., Chairperson

Margaret Phillips, Ph.D.

Joel Goodman, Ph.D.

DEDICATION

To my parents, sister, and friends for their love and support

To my mentor and committee members for their guidance

INSIGHTS INTO THE METABOLIC REGULATION BY
TORC1 IN RESPONSE TO AMINO ACID SIGNALING

by

JUN CHEN

DISSERTATION

Presented to the Faculty of the Graduate School of Biomedical Sciences

The University of Texas Southwestern Medical Center at Dallas

In Partial Fulfillment of the Requirements

For the Degree of

DOCTOR OF PHILOSOPHY

The University of Texas Southwestern Medical Center at Dallas

Dallas, Texas

August 2017

Copyright

by

Jun Chen, 2017

All Rights Reserved

INSIGHTS INTO THE METABOLIC REGULATION BY GATOR1 IN RESPONSE TO AMINO ACID SIGNALING

Jun Chen

The University of Texas Southwestern Medical Center at Dallas, 2017

Supervising Professor: Benjamin P. Tu, Ph.D.

Nutrients provide energy and building blocks for cells to grow and proliferate. Cells need to be able to adapt their metabolism effectively depending on nutrient availability. Target of rapamycin complex 1 (TORC1) is the master regulator of anabolic processes such as protein synthesis, and catabolic processes, such as autophagy, in response to nutrient changes. Although some permeases and regulatory pathways are believed to be involved in its regulation, the exact metabolic mechanism underlying the response to amino acid deficiency is still unclear.

GATOR1/SEACIT, composed of Npr2p-Npr3p-Iml1p, is a known negative regulator of TORC1

in response to nitrogen quality, for example, amino acid availability. The GATOR1/SEACIT null yeast strains, are unexpectedly defective in growth in amino acid depleted minimal medium, despite maintaining high TORC1 activity as indicated by high phosphorylation levels of TORC1 substrates. The discrepancy between TORC1 activity, primarily indicated by the phosphorylation status of translation and transcription factors, and growth in the mutant provides a context to investigate the regulation of metabolism by TORC1.

In the first part of the thesis, I dissect the molecular components of the GATOR1/SEACIT complex and show that the GATOR1/SEACIT complex is associated with GATOR2/SEACAT. The presence of post-translational modifications on individual components of GATOR1/SEACIT appear more important than GATOR2/SEACAT for the association of the two complexes. The GATOR1/SEACIT complex can also physically associate with mitochondrial proteins.

In the second part of the thesis, I report that the metabolic role of GATOR1/SEACIT in response to amino acid starvation is to maintain nitrogen-producing cataplerotic reactions of the mitochondrial TCA cycle to support cell growth and proliferation. I show that the defective growth phenotype of GATOR1/SEACIT mutants in minimal glucose medium is due to insufficient cataplerotic reactions resulting from impaired mitochondrial TCA cycle activity and retrograde response. Growth can be rescued by supplementation of amino acids derived from the TCA cycle intermediates. In particular, aspartate is sufficient to fully rescue the growth of GATOR1/SEACIT mutants while glutamine can partially rescue the growth defect.

TABLE OF CONTENTS

CHAPTER 1. Introduction

TORC1 Signaling and Nitrogen Sensing	1-2
SEACIT/GATOR1 and TORC1	2-4

CHAPTER 2. Molecular Composition of GATOR1/SEACIT

Npr2p is Part of SEA complex and Interacts with Mitochondrial Proteins and Mec1p	7-8
Npr2p “Interactome” Remains Stable in Different Nutrient Conditions	8-10
The GATOR1/SEACIT Complex is Crucial for SEA Complex Formation	11
Npr2p Phosphorylation is Important for the SEA Complex Formation	11-12
Summary	12-13

CHAPTER 3. The GATOR1/SEACIT Complex Regulates Nitrogenic Catabolic

Reactions through TORC1

High TORC1 Activity Induced Growth Defect of <i>npr2Δ</i> Mutants in Minimal Glucose Medium (SD)	22-23
<i>npr2Δ</i> Growth Defect can be Completely Rescued by Aspartate, or Partially Rescued by Glutamine.....	23-25
<i>npr2Δ</i> Mutants Have Defective Mitochondrial Respiration	25-30
<i>npr2Δ</i> Mutants Cannot Activate the Retrograde Response Pathway for Glutamate and Glutamine Synthesis	31-33
<i>npr2Δ</i> Mutants Exhibit Compromised Nucleotide Production.....	33-36
Genetic Screen for Modifiers of GATOR1/SEACIT Function	36-37
Summary	37-42

CHAPTER 4. Material and Methods

Yeast Strains, Gene Deletion and Tagging	72
Yeast Metabolic Cycle	72
Flag Tagged Protein Immunoprecipitation	73
Silver Stain	73
Mass Spectrometry Protein Identification	73-74
Protein Co-immunoprecipitation	74
DNA/RNA Purifications and RT-qPCR	74
Cell Collection, Protein Extraction and Detection	74-75
Phosphatase Treatment	75
Detection of Phosphorylated Sch9 by NTCB Cleavage	75
Phos-tag Gel Electrophoresis	76
Coomassie Blue Staining	76
Cells for Metabolite Extractions	76
Metabolite Analysis by LC-MS/MS	76
Halo Assay	76
¹⁵ N-Ammonium Sulfate or ¹³ C-Glucose or Labeling and Tracer Analysis	77
¹³ C-Acetate Labeling and Tracer Analysis	77
Glucose and NAD ⁺ /NADH Measurements	77
Dissolved Oxygen Level Measurement	77
Live Cell Imaging	78
Hierarchical Clustering Analysis and Heat Maps	78
CHAPTER 5. Bibliography.....	79-85

LIST OF FIGURES

CHAPTER 1. Introduction

Figure 1.1	5
Figure 1.2	6

CHAPTER 2. Molecular Composition of GATOR1/SEACIT

Figure 2.1	14
Figure 2.2	15-16
Figure 2.3	17
Figure 2.4	18
Figure 2.5	19-20

CHAPTER 3. The GATOR1/SEACIT Complex Regulates Nitrogenic Catabolic

Reactions through TORC1

Figure 3.1	43-44
Figure 3.2	45
Figure 3.3	46
Figure 3.4	47
Figure 3.5	48
Figure 3.6	49
Figure 3.7	50
Figure 3.8	51
Figure 3.9	52
Figure 3.10	53
Figure 3.11	54-55

Figure 3.12	56
Figure 3.13	57
Figure 3.14	58
Figure 3.15	59-60
Figure 3.16	61
Figure 3.17	62
Figure 3.18	63
Figure 3.19	64
Figure 3.20	65
Figure 3.21	66
Figure 3.22	67

LIST OF DEFINITIONS

Abbreviation Definition

ATP	Adenosine TriPhosphate
CCCP	Carbonyl Cyanide m-ChloroPhenylhydrazone
CSM	Complete Supplement Mixture
dO ₂	dissolved Oxygen
EDTA	EthyleneDiamineTetraacetic Acid
GATOR1	GAP activity toward Rags
GAP	GTPase activating protein
GEF	Guanine nucleotide exchange factor
GFP	green fluorescent protein
MMP	Mitochondrial Membrane Potential
NAD	Nicotinamide Adenine Dinucleotide
NADH	reduced nicotinamide adenine dinucleotide
NADP	Nicotinamide Adenine Dinucleotide Phosphate
NADPH	reduced nicotinamide adenine dinucleotide phosphate
NCR	Nitrogen catabolite repression
NNS	Non-nitrogen starvation
LC-MS/MS	Liquid chromatography-tandem mass spectrometry
OX	Oxidative
PCR	polymerase chain reaction
PMSF	phenylmethylsulfonylfluoride
qPCR	real-time PCR

RB	Reductive Building
RC	Reductive Charging
ROS	Reactive Oxygen Species
SCD	Synthetic medium with Complete supplement mixture D-glucose
SD	Synthetic medium with D-glucose
SL	Synthetic medium with Lactate
TCA	Trichloroacetic Acid
TCA cycle	Tricarboxylic Acid Cycle (citric acid cycle)
TORC1	Target of Rapamycin complex 1
WT	Wild Type
YPD	Yeast extract Peptone medium with D-glucose
YPD	Yeast extract Peptone medium with Lactate
YMC	Yeast Metabolic Cycle

CHAPTER ONE

INTRODUCTION

TORC1 Signaling and Nitrogen Sensing

The budding yeast *Saccharomyces cerevisiae* regulates cell growth and metabolism in response to nutrient availability through the conserved Target of Rapamycin Complex 1 (TORC1) (Loewith and Hall, 2011). TORC1 in yeast contains the kinase component Tor1p, essential component Kog1p, a highly conserved subunit Lst8p, and Tco89 which is only found in *S. cerevisiae*, *S. pombe*, and *C. albicans*, but not in higher eukaryotes (Loewith et al., 2002; Reinke et al., 2004) (figure 1.1). The *TOR1* and *TOR2* genes were first identified in yeast as mutations led to resistance to the immunosuppressant drug rapamycin (Heitman et al., 1991). *TOR* was later found to be a eukaryotic serine/threonine kinase, evolutionarily conserved from fungi to humans (Thomas and Hall, 1997).

Major targets of TORC1 include Sch9p, Gln3p and Atg13 (figure 1.1). High TORC1 activity induces the phosphorylation of at least 6 residues in Sch9, an AGC family kinase and functional analog of mammalian S6K, which activates ribosome biogenesis and translation initiation for the control of cell growth and longevity (Fabrizio et al., 2001; Huber et al., 2011; Kaeberlein et al., 2005; Urban et al., 2007). Gln3p is a transcriptional activator that promotes the expression of nitrogen catabolite repression (NCR)-sensitive genes required for the assimilation of poor nitrogen sources such as proline or urea (Courchesne and Magasanik, 1988). TORC1 induces the phosphorylation of Gln3p, which promotes the binding of Gln3p to its cytoplasmic anchor Ure2 and

thereby sequesters the transcription factor in the cytoplasm to inhibit NCR (Beck and Hall, 1999). Autophagy is a “self-eating” process in which cytoplasmic and organellar contents are catabolized in the lysosome. TORC1 hyperphosphorylates Atg13 to inhibit the assembly of the Atg1 protein kinase complex, which subsequently prevents autophagy (Kamada et al., 2010).

Nitrogen is essential for the synthesis of amino acids, nucleotides and other cellular compounds. High-quality nitrogen sources can promote cell growth and repress the NCR genes (Magasanik and Kaiser, 2002). TORC1 is responsive to amino acid availability and/or the quality of nitrogen sources to regulate an extensive network of energy-consuming processes important for cell growth and nitrogen assimilation (Diaz-Troya et al., 2008; Nakashima et al., 2008; Urban et al., 2007). Upon amino acid or nitrogen starvation, decreased TORC1 activity triggers autophagy and other metabolic adaptations important for cell survival (Kamada et al., 2010; Loewith and Hall, 2011; Schmidt et al., 1998). Low TORC1 activity during nitrogen starvation results in the dephosphorylation of Gln3p, which enables its nuclear translocation and activation (Cardenas et al., 1999; Crespo et al., 2002). Nitrogen starvation-induced inhibition of TORC1 activity also leads to dephosphorylation of Npr1p, which induces the expression of Gap1p – a general amino acid permease, and negatively regulates Tat1 – a high affinity tryptophan permease (Schmidt et al., 1998).

SEACIT/GATOR1 and TORC1

The conserved, vacuole-associated Rag GTPases Gtr1p and Gtr2p form a heterodimer to control the activity of TORC1 in response to nutrient signals (Binda et al.,

2009; Kim et al., 2008; Sancak et al., 2010). A variety of regulators of TORC1 have been shown to function by modulating the activity of these small GTPases, through their action as GEFs (Guanine nucleotide exchange factors) or GAPs (GTPase activating proteins). One negative regulator complex, named SEACIT in yeast or GATOR1 in mammals, consists of Npr2p, Npr3p and Iml1p (Dokudovskaya et al., 2011; Wu and Tu, 2011), and was identified as a GAP for the Rag GTPases (Bar-Peled et al., 2013; Panchaud et al., 2013) (Figure 1.1). This conserved, vacuole-associated complex functions as a major negative regulator of TORC1 in response to amino acid insufficiency (Neklesa and Davis, 2009).

Npr2p and Npr3p were first identified as “nitrogen permease regulators” in yeast important for growth in poor nitrogen sources (Neklesa and Davis, 2009; Rousselet et al., 1995; Spielwoy et al., 2010). Loss of GATOR1/SEACIT components leads to insensitivity to amino acid starvation (Bar-Peled et al., 2013; Panchaud et al., 2013). The importance of glutamine for the growth and proliferation of a variety of cell types has long been known (Rubin, 1990; Stumvoll et al., 1999; Yuneva et al., 2007). However, the extent through which TORC1 influences other metabolic pathways beyond glutamine metabolism in the regulation of cell growth and homeostasis remain incompletely understood.

Previously, our lab observed that without Npr2p, yeast cells bypass autophagy and continue to grow in minimal medium containing lactate as the carbon source (Sutter et al., 2013; Wu and Tu, 2011). Under such conditions that demand mitochondrial oxidative metabolism, *npr2Δ* mutants synthesize and consume glutamine for the synthesis of nitrogen-containing metabolites, revealing that activation of TORC1

promotes the synthesis and utilization of glutamine to support proliferative metabolism (Laxman et al., 2014).

However, in minimal glucose medium, it has been observed that *npr2Δ* mutants grow poorly in the presence of the most commonly used nitrogen source, ammonium (Laxman et al., 2014; Neklesa and Davis, 2009; Spielewoy et al., 2010). The slow growth of these mutants is unexpected and seemingly inconsistent with its reported function as a negative regulator of TORC1. The discrepancy may be explained by the differences in metabolic states created by different carbon sources. Under glucose conditions, budding yeast cells undergo glucose repression in which multiple genes involved in the use of alternative carbon sources, respiration and gluconeogenesis are repressed by the coordination of signaling pathways and metabolic processes (Kayikci and Nielsen, 2015; Trumbly, 1992). In other words, yeast cells primarily perform glycolysis in glucose medium, whereas they prefer respiration in medium containing lactate (Figure 1.2). Respiring yeast would have increased TCA cycle activity leading to more abundant TCA metabolites for use in cataplerotic biosynthesis reactions such as production of glutamine from α -ketoglutarate. Thus, it is plausible that GATOR1/SEACIT may differentially affect metabolism in response to amino acid starvation in a manner dependent on the carbon source.

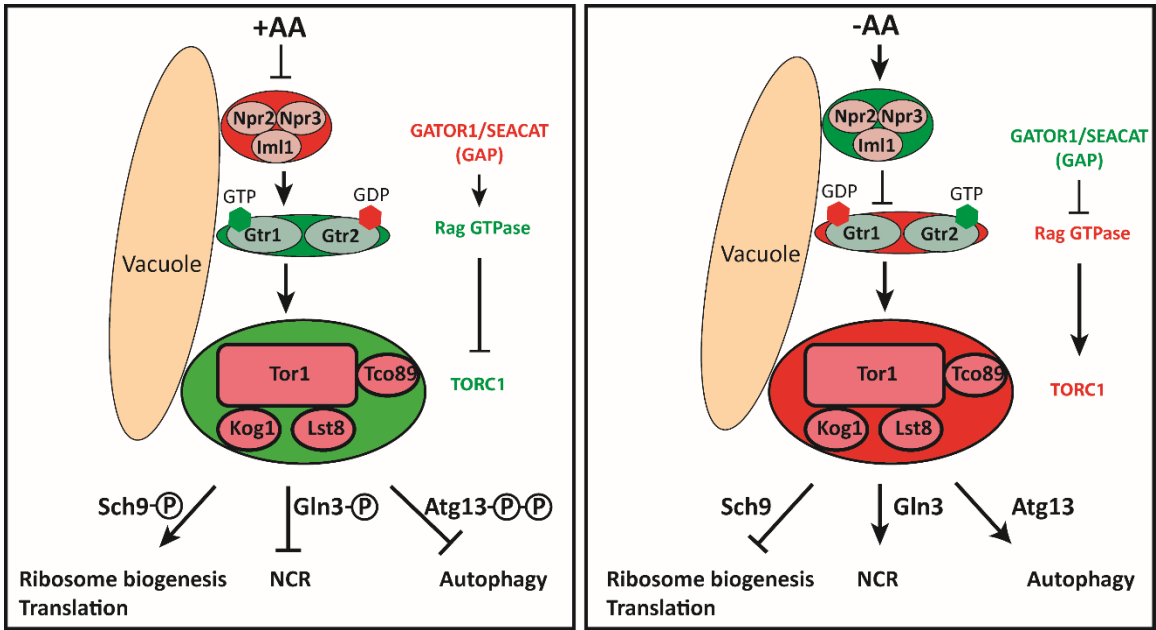


Figure 1.1: GATOR1/SEACIT inhibits TORC1 activity by acting as a GAP for Gtr1-Gtr2 GTPase

TORC1 is composed of Tor1p, Tco89p, Kog1p and Lst8p. When the cell is in a nutrient replete environment, TORC1 is activated and phosphorylates Sch9p for ribosome biogenesis and translation; it also phosphorylates Gln3p to repress nitrogen catabolite repression (NCR) genes and hyper-phosphorylates Atg13p to inhibit autophagy. The activity of TORC1 is controlled by the Gtr1p-Gtr2p heterodimer that act as Rag family GTPases. When the cells are starved for amino acids, the GATOR1/SEACIT complex (Npr2p-Npr3p-Iml1p) will be activated and serves as a GAP to inhibit Gtr1p-Gtr2p, thereby inhibiting TORC1.

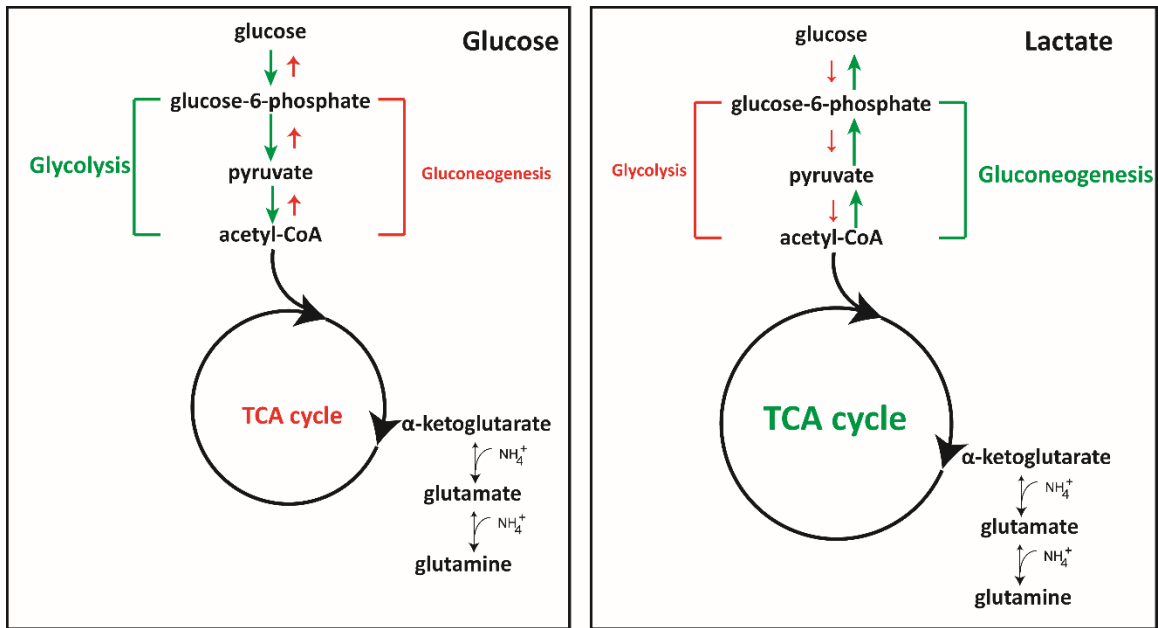


Figure 1.2: Glucose metabolism profile in glucose and lactate medium.

Glucose in the medium induces glucose repression in yeast cells, leading to repression of TCA cycle, respiration, and gluconeogenesis, while increasing glycolysis to generate ATP. When cells are grown in a non-fermentable carbon source, for example, lactate medium, they must boost TCA cycle activity for energy production and also increase gluconeogenesis to produce glucose.

CHAPTER TWO

MOLECULAR COMPOSITION OF GATOR1/SEACIT

Npr2p is Part of SEA Complex and Interacts with Mitochondrial Proteins and Mec1p

The GATOR1/SEACIT (Npr2p-Npr3p-Iml1p) complex was known to interact with Sea2p, Sea3p, Sea4p, Seh1p and Sec13p and together, formed a complex called the SEA complex (Dokudovskaya et al., 2011). Sea2p, Sea3p, Sea4p, Seh1p and Sec13p are coatmer-related proteins with β -propeller/ α -solenoid folds and contain RING domains (Dokudovskaya et al., 2011). Later, they were found to form a complex named GATOR2 or SEACAT and function as a conserved negative regulator of the GATOR1 complex (Bar-Peled et al., 2013; Panchaud et al., 2013) (Figure 2.1A).

To better understand the complex, I aimed to identify additional interacting proteins that might affect the stability of the complex under different conditions, as well as potential post-translational modifications (PTMs). To immunopurify the complex from cells, I tried different tags, including TEV, PrtA, Flag and HA, and different beads and finally came to an optimized pull-down strategy with Flag tag and Dyna beads. To identify the Npr2p-interacting proteins, C-terminal tagged Npr2-flag cells were grown in YPL till log phase, then lysed and pulled down with anti-Flag antibody bound Dyna beads. The beads were then eluted with 3XFlag peptide and the eluted Npr2-interacting proteins were separated by 4-12% SDS-PAGE gel and visualized by silver staining (Figure 2.1B). WT cells with no tag were used as negative control (Figure 2.1B). Mass spec identified dozens of proteins, including all the SEA complex proteins – Npr2p,

Npr3p, Iml1p, Sea2p, Sea3p, Sea4p, Seh1p and Sec13p; as well as heat shock proteins and ribosomal proteins (Table 2.1). Npr2p was also found to interact with mitochondrial proteins, including the mitochondrial outer membrane protein Por1p, cytochrome bc complex proteins Cor1p, Qcr2p, Cyt1p, mitochondrial TCA cycle enzymes Sdh1p and Idh1p, and the mitochondrial phosphate carrier Mir1p (Table 2.1). To confirm the interaction, I tagged Qcr2p with HA tag and showed that Qcr2-HA can be co-immunoprecipitated with Npr2-flag (Figure 2.1C). This potential Npr2p-mitochondrial interaction inspired me to start the second part of the thesis. However, my mass spec result was not exhaustive, since some known interacting proteins such as Gtr1p were not identified (Panchaud et al., 2013). Furthermore, Mec1p, which protects cells from DNA damage and telomere shortening, was found to interact with Npr2p in Co-IP but not in the mass spec data (Figure 2.1D, Table 2.1).

Npr2p “Interactome” Remains Stable in Different Nutrient Conditions

To understand how the GATOR1/SEACIT complex regulates TORC1, I first looked into the stability of the GATOR1 complex and the SEA complex under different nutrient conditions. Yeast can grow in both glucose (fermentable carbon source) and lactate (non-fermentable carbon source), with very different metabolic profiles. To test if the carbon source affects the GATOR1/SEACIT or the SEA complex, I harvested C-terminal tagged Npr2-flag cells in log phase from YPL (rich medium with lactate), YPD (rich medium with glucose) and SD (minimal medium with glucose but no amino acid). The Npr2p interacting proteins were pulled down as mentioned above and resolved with

a 4-12% SDS-PAGE gel. There was no significant difference in the interacting proteins pulled down by Npr2-flag between different media (Figure 2.2A).

Previously, our lab discovered that WT cells underwent non-nitrogen starvation (NNS) induced autophagy when switched from YPL to SL medium, while *npr2Δ* cells bypassed autophagy under such condition (Wu and Tu, 2011). I next tested whether the stability of the SEA complex contributed to NNS induced autophagy. The Npr2-flag cells were grown and harvested from YPL at log phase and transferred to SL and collected at 0.5, 3, 6 hours or overnight. The autophagy level was measured by the dissociation of GFP from the Idh1-GFP strain, which was a consequence of mitophagy. Autophagy occurred at approximately 3 hours after switch (Figure 2.2B). The silver stain of the Npr2-interacting proteins revealed that the switch from YPL to SL did not affect the SEA complex composition, with the exception that Seh1p interaction with Npr2p was much weaker at 0.5 hour after switch into SL (Figure 2.2B).

When yeast cells are grown in a chemostat with steady temperature, controlled pH, and continuous feeding with glucose medium they will become synchronized. Their oxygen consumption, gene expression and metabolome were observed to oscillate in a phenomenon the called yeast metabolic cycle (YMC) (Figure 2.2C) (Tu et al., 2005). The YMC is very useful for the study of how cellular processes are coordinated with growth phase or metabolic status. The cycle is divided into 3 phases, OX (oxidative), RB (reductive building) and RC (reductive charging) phases, each is linked to different growth phases and different metabolic profiles (Figure 2.2C) (Tu et al., 2005). For OX phase, cells are in growth phase and rapidly consume oxygen for ribosome biogenesis; For RB phase, cells start to divide; For RC phase, cells consume very little oxygen and

enter a G0-like phase, expressing stress genes including heat shock proteins and autophagy components (Tu et al., 2005).

I collected Npr2-flag cells from one YMC cycle with one representative time point for each phase (Figure 2.2C). WT cells in the same time point for OX phase were used as a negative control. The Npr2p-interacting proteins were resolved on an 8% homemade gel and compared in parallel. There was no significant difference between different conditions except that the Seh1p interaction was lost at RC phase (Figure 2.2C).

Since cells in RC phase induce autophagy genes, and Seh1p interaction with Npr2p is reduced in early YPL to SL switch, also an autophagy inducing condition (Figure 2.2B), the Seh1p-Npr2p interaction may play a role in autophagy induction. To test this possibility, I made a *seh1Δ* strain in the Idh1-GFP background and compared the level of NNS induced autophagy between WT and *seh1Δ* (Figure 2.3A). Interestingly, *seh1Δ* strain underwent autophagy in rich medium YPL before amino acid starvation (Figure 2.3A). This provided further evidence for the opposing roles of Seh1p and Npr2p in the regulation of NNS autophagy. To understand how Npr2p regulates Seh1p, I compared the PTM of Seh1p between WT and *npr2Δ* backgrounds (Figure 2.3B). Seh1-HA cells were collected from YPL or switched to SL. The Seh1p protein isolated from *npr2Δ* cells migrated at an apparently higher molecular weight during SDS-PAGE compared to Seh1p from WT cells, regardless of the nutrient condition. Phosphatase treatment of the protein extracts had no effect on the shift, indicating that the shift was not caused by phosphorylation (Figure 2.3B). It is possible that this modification on Seh1p is the key downstream switch that controls NNS induced autophagy since *npr2Δ* cells are unable to undergo NNS induced autophagy.

The GATOR1/SEACIT Complex is Crucial for SEA Complex Formation

To examine the importance of individual SEA complex proteins, I made a knockout of each protein in the Npr2-flag background and compared the profiles of Npr2p-interacting proteins. Npr3p and Iml1p were both essential for the SEA complex, since Npr2-flag cannot pull down the rest of the SEA complex from *npr3Δ* and *iml1Δ* strains grown in both YPL and SL medium (Figure 2.4A). Npr2p bound tightly to Npr3p, since Npr3p was observed in the silver stain in *iml1Δ*. Npr3p is important for the formation of GATOR1/SEACIT since Iml1p cannot be pulled down by Npr2p in *npr3Δ* mutants (Figure 2.4A). These data were consistent with previous co-IP experiments (Wu and Tu, 2011). None of the individual knock-outs of Sea2p, Sea3p or Sea4p prevented the Npr2-flag from pulling down the rest of the SEA complex proteins, however, there was a slight size difference in Seh1p in *sea2Δ* (Figure 2.4B). Therefore, the individual components of GATOR2/SEACAT do not appear critical for the SEA complex assembly.

Npr2p Phosphorylation is Important for the SEA Complex Formation

Previous studies in the lab showed that Npr2p is heavily phosphorylated in YPL and appears as two bands in an SDS-PAGE gel (Wu and Tu, 2011). Dephosphorylated Npr2p was known to interact with Npr3p but not Iml1p (Wu and Tu, 2011). My data suggested that the loss of Npr2p-Iml1p interaction disrupted the SEA complex (Figure 2.4A). The level of Npr2p phosphorylation varies among different medium conditions, with more phosphorylation occurring in less favorable medium. Thus, the phosphorylation of Npr2p may be key to the regulation of the SEA complex. A previous student in the lab used mass spectrometry to identify potential phosphorylation

sites in Npr2p in YPL and decided to mutate 5 phosphorylation sites (S262, S275, S312, S318 and S319) to alanine to make the Npr2(5SA)p mutant, which is expected to behave as a phosphomutant (Figure 2.5A).

I intended to use the Npr2(5SA)p mutant to study the importance of Npr2p phosphorylation on the assembly of SEA complex. The Npr2(5SA)p migrated comparably to dephosphorylated Npr2p on an SDS-PAGE gel, and interacted with Npr3p, but not Iml1p, during the YPL to SL switch (Figure 2.5B). Taken together, the Npr2(5SA)p mutant behaved like dephosphorylated Npr2p using multiple assays. I then examined the interacting protein profiles by pull down experiments. Since the Npr2(5SA)p does not bind to Iml1p (Figure 2.5B), it is not surprising to find out that the Npr2(5SA)p mutant does not form the SEA complex in the YPL to SL switch (Figure 2.5C), and therefore cannot pull down Seh1p (Figure 2.5D). Since the pull down results were so similar to *npr3Δ* or *iml1Δ*, I decided to test autophagy and growth of the Npr2(5SA)p mutant. The Npr2(5SA)p mutant indeed behaved like an *npr2Δ* mutant, with faster growth (Figure 2.5E) and no NNS induced autophagy (Figure 2.5F).

Summary

My experiments aimed to characterize the structural and functional organization of the yeast Npr2p-containing SEA complex. Npr2p, Npr3p and Iml1p (members of the GATOR1/SEACIT) are crucial for the stability of the SEA complex, while each of the GATOR2/SEACAT (Sea2p, Sea3p, Sea4p, Seh1p and Sec13p) components did not notably impact SEA complex formation. My findings were consistent with a paper published later in 2014 (Algret et al., 2014), which proposed a structure of the SEA complex using a computational model (Algret et al., 2014). The Npr2p-

mitochondrial interaction was also reproducible in their mass spec analysis, providing a potential explanation for the crosstalk between TORC1 and mitochondria.

The SEA complex appears to be a very stable complex that barely dissociates in most medium conditions. The Seh1p dissociates from the complex during the initial stages of the Npr2-regulated autophagy, which indicates a potential role of the Seh1p-Npr2p interaction for initiation of autophagy. As a member of the nuclear pore complex, Seh1p reportedly interacts with ~20% of yeast genes, potentially providing a wide range of regulation by Npr2p (Costanzo et al., 2010; Siniossoglou et al., 1996).

Phosphorylation of Npr2p was shown to be important for interaction with Iml1p (Wu and Tu, 2011), and therefore key to the regulation of the SEA complex and the GATOR1/SEACIT complex. Our best serine to alanine mutant (Npr2(5SA)) behaved like a knockout, supporting the idea that phosphorylation is required for Npr2p to inhibit GATOR1/SEACIT function. However, the phosphorylation of Npr2p might be more complicated than originally anticipated. One complication to our studies of Npr2 phosphorylation thus far was due to our inability to construct a successful phosphomimetic for further mechanistic study.

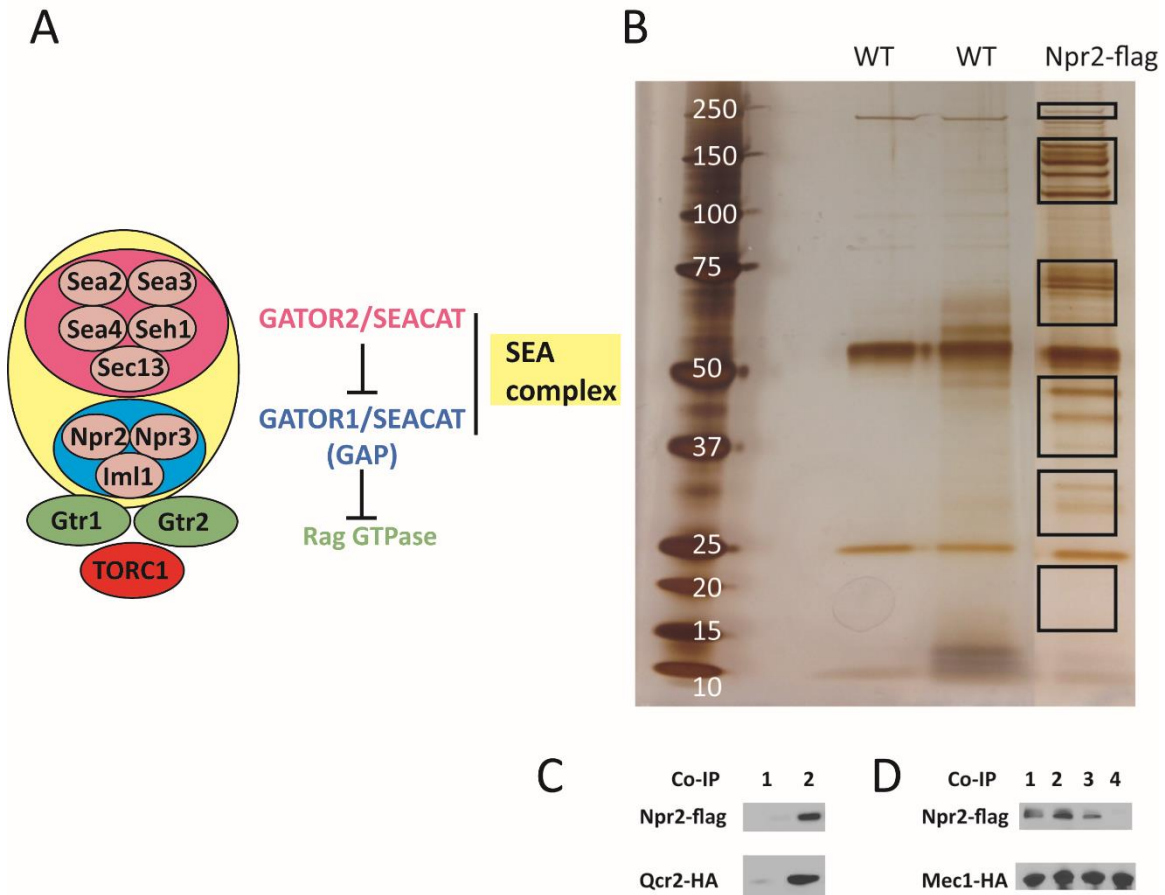


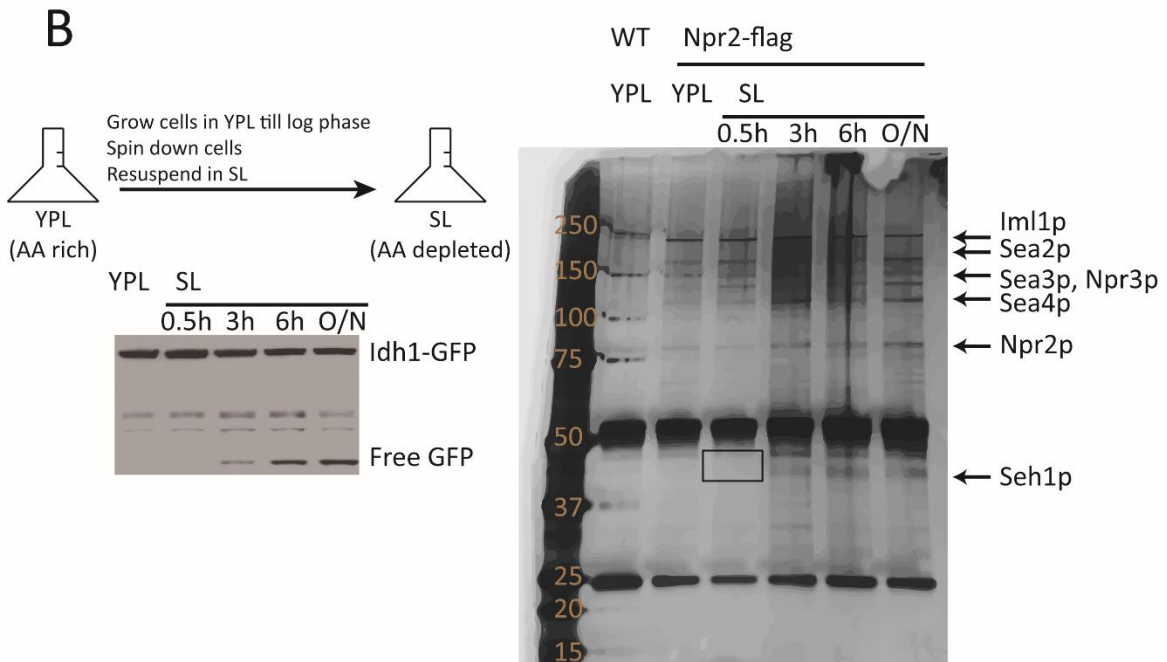
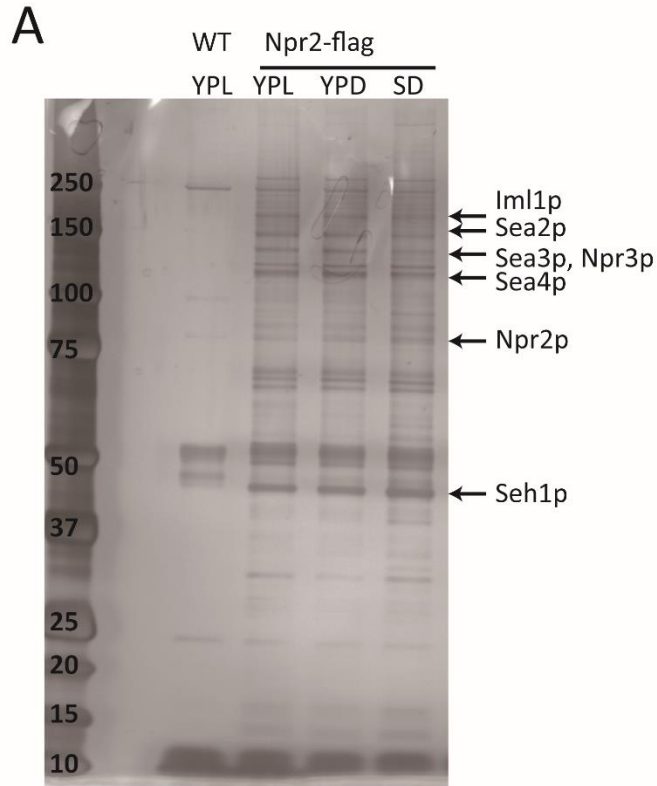
Figure 2.1 Npr2p is part of the SEA complex and interacts with mitochondrial proteins and Mec1p

A) Npr2p forms the SEA complex, which contains 2 sub-complexes: GATOR1/SEACIT (Npr2p, Npr3p, Iml1p) which acts as a GAP to inhibit Gtr1-Gtr2 heterodimeric GTPase, thereby, inhibiting TORC1; and GATOR2/SEACAT (Sea2p, Sea3p, Sea4p, Seh1p, Sec13p) which inhibits GATOR1/SEACIT, therefore, activating TORC1.

B) Silver stain of Npr2p-interacting proteins for mass spec analysis. The interacting proteins were resolved using a 4-12% gel. The boxes label the gel sections containing Npr2-interacting proteins sent for mass spec ID. The significant results were shown in table 2.1.

C) Western blot showing the interaction between Npr2p and the mitochondrial protein Qcr2p. 1: Qcr2-HA, served as a negative control. 2: Npr2-flag, Qcr2-HA. Npr2-flag was immunoprecipitated from YPL at log phase from the indicated strains and probed with anti-HA to detect Qcr2.

D) Western blots showing the interaction between Npr2p and Mec1p. 1: Mec1-HA, Npr2-Flag 2: Mec1-HA, Npr2-flag, *npr3Δ*. 3: Mec1-HA, Npr2-flag, *iml1Δ*. 4: Mec1-HA, served as a negative control. Npr2-flag was immunoprecipitated from YPL at log phase from the indicated strains and probed with anti-HA to detect the interacting Mec1p.



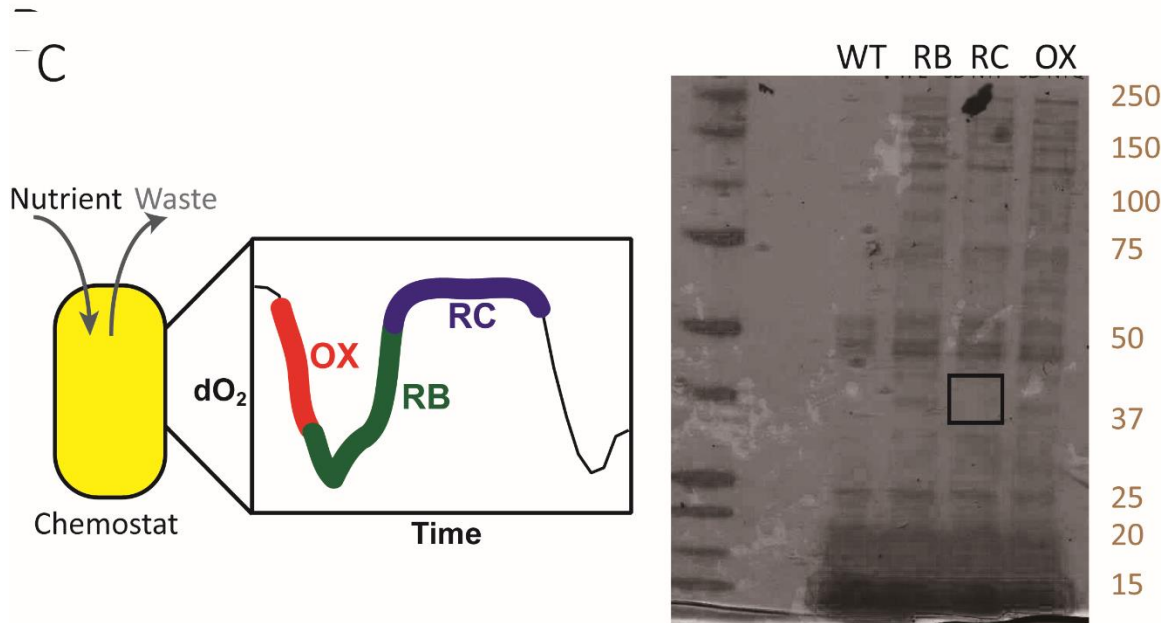


Figure 2.2 The SEA complex remains stable in different nutrient conditions

- A) Silver stain of Npr2p-interacting proteins collected from YPL, YPD and SD. WT: wild type cells with no tag, served as negative control. Npr2-flag: Npr2p C-terminal tagged. Npr2-flag was immunoprecipitated from indicated medium at log phase with anti-flag antibody and then eluted with 3XFlag peptide. The interacting proteins were resolved using a 4-12% gel.
- B) Silver stain of Npr2p-interacting proteins from YPL to SL switch. GFP cleavage assay from Idh1-GFP was used as a measure of mitophagy during the switch (left). Free GFP indicates that autophagy was happening. The interacting proteins at each time point were resolved on a 4-12% gel (right). Seh1p interaction was significantly less in SL at 0.5 hour (boxed).
- C) Npr2-flag cells were collected at the indicated representative time points for OX, RB and RC phase from one YMC. The interacting proteins were resolved on an 8% gel (right), WT from OX phase was used as negative control. Seh1p interaction was significantly less in RC (boxed).

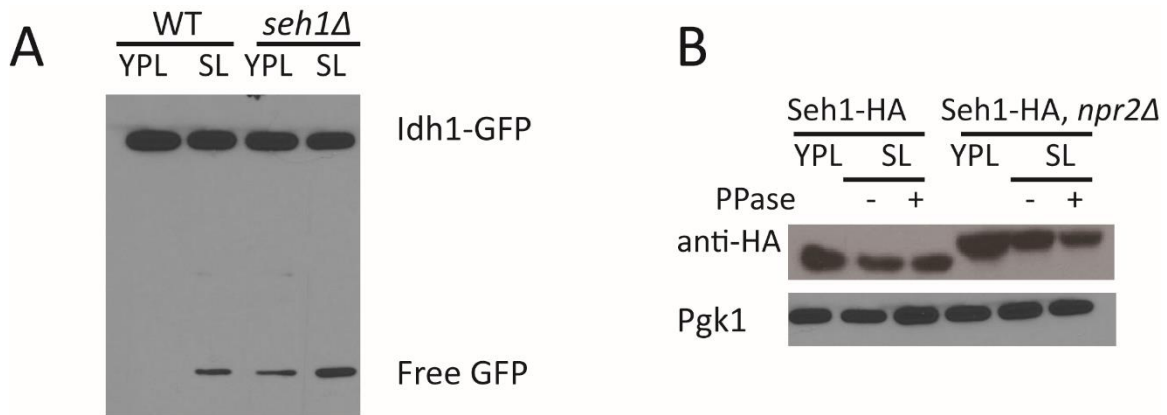


Figure 2.3: Seh1p is involved in Npr2-regulated NNS autophagy.

A) Autophagy assay for *seh1Δ* from YPL to SL switch. Cells were grown in YPL until log phase then transferred to SL for 6 hours. *seh1Δ* cells induced autophagy even in rich medium YPL.

B) Western blots of Seh1-HA collected from YPL to SL switch. Cells were grown in YPL until log phase and then transferred to SL for 6 hours and split into two, one treated with phosphatase (PPase +), the other remained untreated (PPase -).

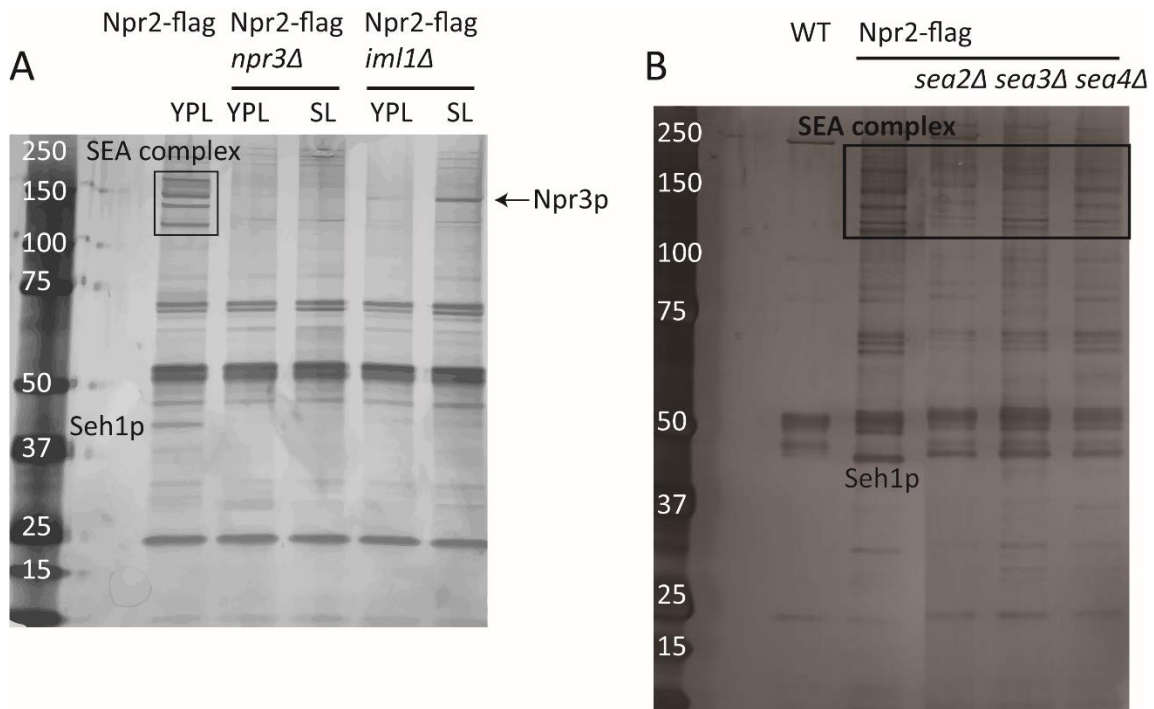


Figure 2.4: GATOR1/SEACIT components are important for SEA complex formation.

A) Silver stain of Npr2p-interacting proteins in *npr3Δ* or *iml1Δ* background. Npr2-flag, *npr3Δ* or Npr2-flag, *iml1Δ* cells were collected from YPL at log phase and transferred to SL for 3 hours. The SEA complex components (boxed area together with Seh1p at lower molecular weight area) were absent in the *npr3Δ* or *iml1Δ* background.

B) Silver stain of Npr2p-interacting proteins in *sea2Δ*, *sea3Δ* or *sea4Δ* background. Cells were collected from YPL at log phase. The absence of these GATOR2 components did not affect the general SEA complex (boxed area).

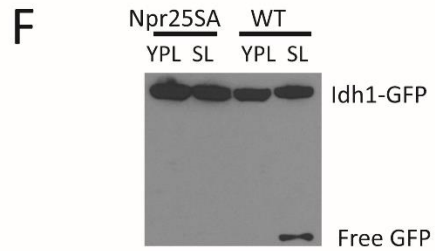
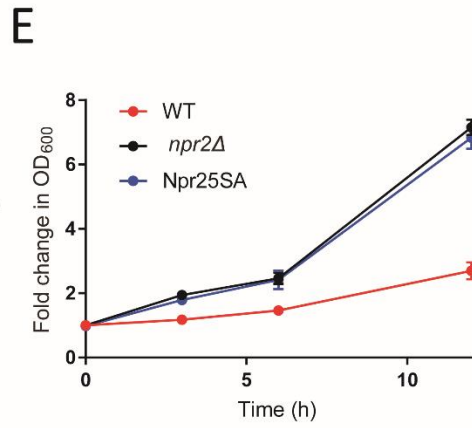
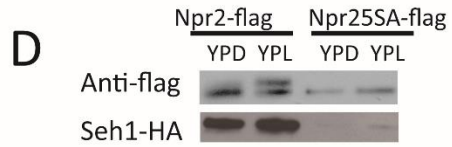
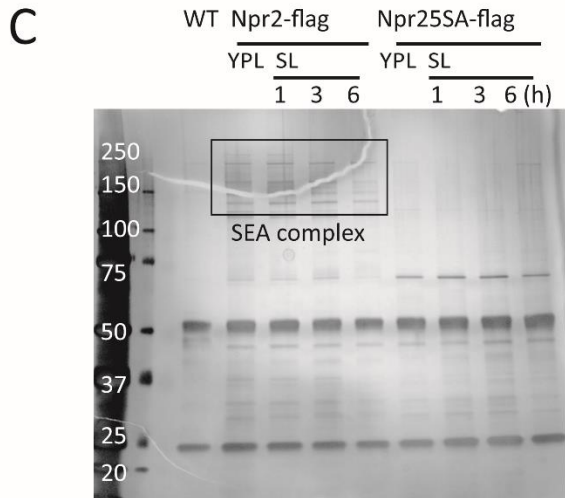
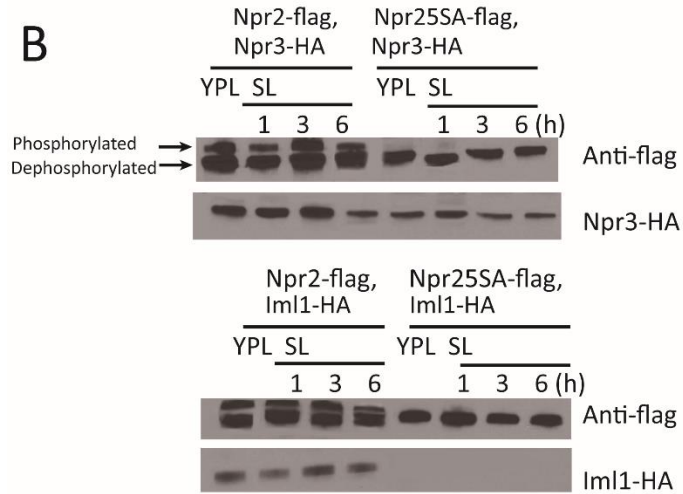
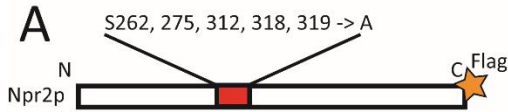


Figure 2.5: Phosphorylation of Npr2p is important for SEA complex formation

A) Construct of Npr2(5SA)-flag: 5 serine residues (S262, S275, S312, S318 and S319) were mutated to alanine, the mutant mimics dephosphorylated Npr2, C-terminal flag tagged.

B) Western blots showing the interaction between Npr2p or Npr2(5SA) and Iml1p and Npr3p in YPL to SL switch. Npr2-flag or Npr2(5SA)-flag was immunoprecipitated from indicated conditions and probed with anti-HA to detect interacting Npr3p (upper) or Iml1p (lower).

C) Silver stain of Npr2p-interacting proteins collected from YPL to SL switch. Npr2-flag was immunoprecipitated from indicated conditions with anti-flag antibody and then eluted with 3XFlag peptide. The interacting proteins were resolved in a 4-12% gel. Interaction with SEA complex (boxed area) was absent in the Npr2(5SA) mutant.

D) Western blots showing the interaction between Seh1p and Npr2p or Npr2(5SA) mutant in YPD or YPL. Npr2-flag or Npr2(5SA)-flag was immunoprecipitated from YPL or YPD at log phase and probed with anti-HA to detect interacting Mec1p.

E) Growth curve of WT, *npr2Δ* and Npr2(5SA) in SL. Cells were grown in YPL until log phase then switched to SL to measure the growth rate indicated by OD₆₀₀. Data were collected from 3 independent experiments.

F) Autophagy assay for Npr2(5SA) from YPL to SL switch. Cells were grown in YPL until log phase then transferred to SL for 6 hours.

Standard Name	Systematic Name	Description
NPR2	YEL062W	Nitrogen Permease Regulator, Iml1p/SEACIT complex
IML1	YJR138W	GTPase-activating protein (GAP) subunit of the Iml1p/SEACIT complex
NPR3	YHL023C	Nitrogen Permease Regulator, Iml1p/SEACIT complex
RTC1 (SEA2)	YOL138C	Restriction of Telomere Capping
MTC5 (SEA3)	YDR128W	Maintenance of Telomere Capping
SEA4	YBL104C	SEh1 Associated
SEH1	YGL100W	SEc13 Homolog
SEC13	YLR208W	Structural component of 3 complexes: Nup84, COP II complex, SEA complex
SSA1	YAL005C	ATPase involved in protein folding and NLS-directed nuclear transport; member of HSP70 family
HSP60	YLR259C	Tetradecameric mitochondrial chaperonin
TEF1	YPR080W	Translational elongation factor EF-1 alpha
MIR1	YJR077C	Mitochondrial phosphate carrier
POR1	YNL055C	Mitochondrial porin (voltage-dependent anion channel)
SDH1	YKL148C	Flavoprotein subunit of succinate dehydrogenase
QCR2	YPR191W	Subunit 2 of ubiquinol cytochrome-c reductase (Complex III)
COR1	YBL045C	Core subunit of the ubiquinol-cytochrome c reductase comple
IDH1	YNL037C	Subunit of mitochondrial NAD(+)-dependent isocitrate dehydrogenase
CYT1	YOR065W	Cytochrome c1
RPL4B	YDL133C-A	Ribosomal 60S subunit protein L41B
TDH1	YJL052W	Glyceraldehyde-3-phosphate dehydrogenase (GAPDH), isozyme 1
DED1	YOR204W	ATP-dependent DEAD (Asp-Glu-Ala-Asp)-box RNA helicase
RPP0	YLR340W	Ribosomal Protein P0

Table 2.1: Mass spec ID result of Npr2-flag pull-down.

The Npr2-interacting proteins were pulled down from YPL at log phase with anti-Flag antibody and separated by a 4-12% gel as shown in Figure 2.2 and ID'd by the core facility. All the SEA complex proteins were identified in the experiment and labeled in yellow. The Npr2-interacting mitochondrial proteins were labeled in red.

CHAPTER THREE

THE GATOR1/SEACIT COMPLEX REGULATES NITROGENIC CATAPLEROTIC REACTIONS THROUGH TORC1

High TORC1 Activity Induced Growth Defect of *npr2*Δ Mutants in Minimal Glucose Medium (SD)

In minimal lactate medium, *iml1*Δ, *npr2*Δ, and *npr3*Δ mutants that lack GATOR1/SEACIT function grow faster than WT cells, consistent with the role of this complex as a negative regulator of TORC1 (Laxman et al., 2014; Sutter et al., 2013). However, in the more commonly used minimal glucose medium (SD), *npr2*Δ, *iml1*Δ, and *npr3*Δ mutants grew notably slower than WT (Figure 3.1A).

To decipher the discrepancy between the growth phenotypes, I first tested if the growth defect was really caused by *NPR2* deletion instead of unknown random or compensatory mutations. I reintroduced a construct expressing *NPR2*-flag into the *npr2*Δ mutant strain (*npr2*Δ, *Npr2*-flag). The strain had normal growth, suggesting that *Npr2*p deletion is the specific reason for the retarded growth in SD medium (Figure 3.1B).

Secondly, I wanted to assess whether *npr2*Δ mutants really had high TORC1 activity in SD. Rapamycin is a potent and specific TORC1 inhibitor. The growth defect of *npr2*Δ, *iml1*Δ, and *npr3*Δ mutants could be rescued by low concentrations of rapamycin, 2 nM for liquid culture or 1 nM for agar plate (Figure 3.1C), while higher concentrations of rapamycin inhibited cell growth of all genotypes (data not shown). This indicated that the *npr2*Δ, *iml1*Δ, and *npr3*Δ mutants had high TORC1 activity, and the high TORC1 activity was the reason for the growth defect. To further support this

possibility, I used a GTP-locked mutant of Gtr1p (Gtr1-Q65L) that has constitutively activated TORC1 (Nakashima et al., 1999). Gtr1-Q65L also grew poorly, similar to the *npr2Δ* mutant (Figure 3.1D). Deletion of *GTR1* alleviated the slow growth phenotype of *npr2Δ* mutants, consistent with the finding that Npr2p functions specifically through Gtr1p to inhibit TORC1 (Figure 3.1D) (Panchaud et al., 2013). Then I determined the phosphorylation levels of the hallmark TORC1 substrates Sch9p, Gln3p and Npr1p to further examine the activity of TORC1 (Cooper, 2002; Schmidt et al., 1998; Urban et al., 2007). *npr2Δ* mutants had more phosphorylated Gln3p and Npr1p in SD compared to WT, which is an indicator of high TORC1 activity in response to a good nitrogen source (Figure 3.1E). However, Sch9p, a reported ortholog of mammalian S6K and major substrate of TORC1 (Urban et al., 2007), became less phosphorylated in *npr2Δ* mutants in SD medium (NTCB-treated Sch9-HA blot and phospho-S6 blot, Figure 3.1E). Taken together, multiple lines of evidence indicate that *npr2Δ* mutants had increased TORC1 signaling, as reflected by the regulation of nitrogen assimilation pathways, but still exhibited defective growth and translation in minimal glucose medium.

***npr2Δ* Growth Defect can be Completely Rescued by Aspartate, or Partially Rescued by Glutamine**

Why would a cell with hyperactive TORC1 signaling grow more slowly? SD medium contains ammonium (NH_4^+) as the sole nitrogen source, requiring prototrophic yeast cells to synthesize all twenty amino acids using ammonium. *npr2Δ* mutants in glucose might perceive themselves to be in an amino acid and nitrogen-replete state, regardless of the nutrient environment. Consistent with this idea, the poor growth of

npr2Δ mutants in SD medium was rescued upon supplementation of a standard amino acid mixture (CSM) (Figure 3.2A). Therefore, *npr2Δ* mutants may inappropriately repress metabolic activities, such as the synthesis of amino acids, because they perceive themselves to already be amino acid-replete. Thus, growth deficits may emerge, especially under conditions that require the synthesis of amino acids (e.g., minimal SD medium).

I next tried to rescue the growth of *npr2Δ* mutants by supplementation of single amino acids into SD medium. Strikingly, the sole addition of modest concentrations of aspartate (2 mM) could completely rescue the growth of *npr2Δ* cells (Figure 3.2B). Glutamine could partially rescue growth of *npr2Δ*, *iml1Δ* and *npr3Δ* cells, but increasing concentrations did not have an additional benefit (Figure 3.2C). Asparagine also fully rescued the growth of *npr2Δ* mutants while methionine only had a partial effect. Other amino acids had no observable effect on growth (Figure 3.2D). Interestingly, the branched-chain amino acids, leucine and isoleucine, modestly inhibited the growth of WT but not *npr2Δ* cells (Figure 3.2D), which may be another layer of evidence that high TORC1 activity in SD hampers cell growth. These rescue experiments suggest that *npr2Δ* mutants might exhibit defects in the synthesis of particular amino acids, especially aspartate, and to a lesser extent, glutamine.

To further understand the metabolic basis of the slow growth of *npr2Δ* mutants in minimal SD medium without amino acids, I measured the relative abundance of intracellular metabolites in *npr2Δ* and WT cells by LC-MS/MS. Focusing first on amino acids, glutamine, glutamate and aspartate amounts were extremely low in *npr2Δ*, as well as in *npr3Δ*, *iml1Δ*, and GTR1 Q65L cells compared to WT (Fig. 3.3), consistent with the

observation that glutamine and aspartate could rescue their growth. These results suggest that the GATOR1/SEACIT complex might play a role in the regulation of glutamine and aspartate synthesis, which led to further investigation of the pathways required for their production.

***npr2*Δ Mutants Have Defective Mitochondrial Respiration**

Glutamine can be synthesized from the TCA cycle intermediate α -ketoglutarate by the sequential actions of glutamate dehydrogenase (Gdh1p/Gdh3p) and glutamine synthetase (Gln1p). Aspartate can be synthesized from the TCA cycle intermediate oxaloacetate, by the action of the aspartate aminotransferases (Aat1p/Aat2p). Since both glutamine and aspartate can be derived from TCA cycle metabolites, I investigated whether mitochondrial functions might be regulated by Npr2p and thus the GATOR1/SEACIT complex.

To assess mitochondrial activity, I first compared the oxygen consumption rate by measuring the level of dissolved oxygen in the medium. From exponential growth to the diauxic shift, I observed that *npr2*Δ and other GATOR1/SEACIT mutants, as well as the GTR1 Q65L mutant, consumed much less oxygen compared to WT during growth in SD medium (Figure 3.4A). Notably, aspartate supplementation did not restore the reduced respiratory activity of *npr2*Δ cells (Figure 3.4A), despite its ability to fully rescue the growth of *npr2*Δ cell (Figure 3.2B, Figure 3.4B). Glutamine supplementation also did not rescue the respiratory activity of *npr2*Δ cells (Figure 3.4A).

Under all conditions tested thus far, I observed the phenotypes of the *iml1*Δ, *npr2*Δ, and *npr3*Δ mutants to be identical (Figure 3.1A, C, D, Figure 3.2 B, C, Figure 3.3

and Figure 3.4A). In subsequent experiments, I focused on the *npr2Δ* mutant to assess the consequences of loss of GATOR1/SEACIT function.

Next, I quantified the mitochondrial content in the cell to determine if the decreased activity was due to loss of mitochondrial mass. The *npr2Δ* mutant had comparable amounts of mitochondria compared to WT as assessed by mtDNA content (Figure 3.4B). Thus, I reasoned the decreased oxygen consumption must be due to a decrease in individual mitochondrial activity of *npr2Δ* cells.

Even though WT cells respire more in SD medium, WT and *npr2Δ* cells consumed glucose at similar rates since glucose was depleted from the medium at similar rates (Figure 3.5A). Therefore, *npr2Δ* cells consume less oxygen per glucose under these conditions, suggesting that *npr2Δ* cells favored glycolysis over aerobic respiration for glucose metabolism. To further investigate the basis of altered respiration, I next examined the TCA cycle activity. I examined TCA cycle enzyme levels and found that *npr2Δ* cells express significantly reduced amounts of most TCA cycle enzymes, including Aco1p, Cit1p, Kgd1p, Sdh1p, Fum1p and Mdh1p (Figure 3.5B).

I measured the corresponding TCA cycle metabolites. However, when compared at similar growth stages, there was no significant difference in TCA cycle metabolite levels between WT and *npr2Δ* cells, except for α -ketoglutarate (Figure 3.6A). Oxaloacetate is not stable at room temperature so it was not measured. The low α -ketoglutarate in *npr2Δ* cells seems to fit our hypothesis that the defective TCA cycle activity of *npr2Δ* cells limits the production of glutamine and other amino acids. However, adding cell-permeable α -ketoglutarate (dimethyl 2-oxoglutarate) was unable to rescue the growth of the mutant (Figure 3.6B). Cells were able to take up dimethyl 2-

oxoglutarate since it largely restored α -ketoglutarate levels of *npr2* Δ cells to comparable levels as WT cells (Figure 3.6C). The failure of α -ketoglutarate rescue indicated that the metabolic pathways downstream of α -ketoglutarate, either following the TCA cycle towards oxaloacetate or towards amino acid synthesis including glutamate and glutamine, are not active enough to effectively support the growth of *npr2* Δ cells.

Bulk measurement of metabolite pools does not inform about the rates of synthesis or consumption. I then developed a mass spec method for D-glucose- $^{13}\text{C}_6$ labeling to assess rates of TCA cycle metabolite production. WT and *npr2* Δ cells consumed similar amounts of glucose over the time period examined (Figure 3.5A). The difference in cell number between WT and *npr2* Δ cells during the labeling period (1 hour) was negligible. Thus, there was no need to normalize the signal against total glucose uptake. Cells were grown in normal medium to the same OD, then switched to medium with D-glucose- $^{13}\text{C}_6$ as the only carbon source. After entering the cell, D-glucose- $^{13}\text{C}_6$ is converted into labeled pyruvate. There are two ways for the labeled pyruvate to enter the TCA cycle. It can be converted either to acetyl-CoA with a loss of one carbon as CO_2 , or carboxylated to oxaloacetate with a gain of one carbon. The ^{13}C -labeling patterns of metabolites from each pathway were assessed as described previously (Buescher et al., 2015; Sugiura et al., 2016). The ^{13}C -labeled metabolites were normalized against the total corresponding metabolite (labeled + unlabeled). For the pyruvate to citrate pathway, *npr2* Δ cells produced significantly less early TCA cycle metabolites (isocitrate and α -ketoglutarate), glutamine and aspartate, throughout a period of 1 hour (Figure 3.7). Considering the difference in total glutamine and aspartate between WT and *npr2* Δ cells (Figure 3.3), the absolute differences between the production of these metabolites were

substantial. For the pyruvate to oxaloacetate pathway, *npr2Δ* cells also produced less glutamine and aspartate from this route (Figure 3.7), despite comparable labeling of most TCA cycle intermediates. Interestingly, the data also suggested that the pyruvate to oxaloacetate pathway is the major aspartate biosynthesis pathway in the cell as more than 20% of the total aspartate was labeled from this pathway, compared to 5% from the pyruvate to citrate pathway. These data suggest that *npr2Δ* mutants are compromised in their ability to synthesize glutamine and aspartate from TCA cycle intermediates.

Since *npr2Δ* cells appear deficient in metabolic activities required for proliferation, I next determined whether *npr2Δ* mutants exhibited hallmarks of oxidative metabolism characteristic of differentiated or non-proliferating cells. The amount of the glutamate synthase enzyme Glt1p was markedly reduced in *npr2Δ* cells, consistent with the idea that these mutants inappropriately perceive themselves to be glutamate or nitrogen-replete (Valenzuela et al., 1998) (Figure 3.8A). Upon examining the enzymes directly involved in aspartate synthesis, pyruvate carboxylase enzyme (Pyc1/Pyc2) amounts were comparable to WT, but amounts of the aspartate aminotransferase enzyme Aat2p were higher in *npr2Δ* cells (Figure 3.8B). The expression profile of AAT2 is correlated with mitochondrial biogenesis, as opposed to growth, across the yeast metabolic cycle (Figure 3.8C), suggesting this particular enzyme is typically induced to promote oxaloacetate synthesis to support mitochondrial activities. In addition, the pyruvate dehydrogenase complex (Pda1p) was significantly less phosphorylated in *npr2Δ* cells, suggesting they prefer the routing of pyruvate into acetyl-CoA for oxidation in the mitochondria (Figure 3.8B). Consistent with this idea, *npr2Δ* cells also expressed higher amounts of the respiratory mitochondrial pyruvate carrier subunit Mpc3p (Figure 3.8B)

(Bender et al., 2015). Taken together, these data all support the idea that mutants lacking GATOR1/SEACIT function perceive themselves to be amino acid and nitrogen-replete, and are wired in a state that favors utilization of the mitochondria for oxidation of glucose-derived pyruvate, instead of aspartate and glutamine synthesis.

Furthermore, *npr2Δ* cells also exhibited a modest reduction in the NAD⁺/NADH ratio, consistent with reduced TCA cycle and respiratory activity (Figure 3.9A). However, supplementation with pyruvate or malate, which could help restore the NAD⁺/NADH ratio (Williamson et al., 1967), could not rescue the growth defect of *npr2Δ* cells (Figure 3.9B).

Notably, substantial amounts of acetate accumulated in the SD medium of *npr2Δ* cells, suggesting a deficiency in acetate utilization for mitochondrial functions (Figure 3.10A). To test this possibility, I used a mass spec method for acetate-¹³C₂ tracing to assess the acetate metabolism in the cell. Compared with the glucose concentration in the SD medium (~111 mM), the acetate-¹³C₂ concentration for tracing (2 mM) was small and unlikely to perturb general carbon metabolism. Thus, the method can be used to measure the acetate metabolism in SD. One limitation of the small amount of the tracer is that the signals were not ideal - only 2 labeled metabolites were detected: ¹³C-cis-aconitate (TCA metabolite, intermediate of citrate and isocitrate) and ¹³C-glutamate. Again, the isotope-labeled metabolites were normalized against total corresponding metabolites. The *npr2Δ* cells had less TCA metabolite (¹³C-cis-aconitate) and glutamate production from acetate (figure 3.10B). Therefore, not only do *npr2Δ* mutants appear wired for mitochondrial oxidative metabolism, they also have defects in the actual utilization of the TCA cycle for mitochondrial acetate metabolism.

To assess the consequences of the skewed oxidative metabolism, I compared the growth under reactive oxygen species (ROS) stress using the H₂O₂ halo assay. The *npr2Δ* cells were more sensitive to oxidative stress induced by H₂O₂ on SD plates (Figure 3.11A). The respiratory chain reaction pumps protons across the mitochondrial inner membrane and creates the mitochondrial membrane potential (MMP) for ATP synthesis. The MMP is the major source of ROS stress in the cell (Korshunov et al., 1997). Thus, MMP measurements can be useful for investigating ROS and TCA cycle activity.

I used the MitoMap plugin in ImageJ to assess the mitochondrial network volume and MitoLoc to assess the MMP intensity (Vowinckel et al., 2015). Dioc6 (3,3'-dihexyloxycarbocyanine iodide) is a dye for mitochondria, and the fluorescent intensity is related to MMP (Koning et al., 1993; Perry et al., 2011). MMP increased upon switch from YPD to SD (Figure 3.11B), consistent with the idea that upon amino acid starvation, cells need to increase TCA cycle activity for the synthesis of nitrogenous metabolites. However, *npr2Δ* cells were slow at increasing the MMP at an early time point (1 hour) after starvation (Figure 3.11B). This again showed that *npr2Δ* cells were tricked into thinking they are nutrient replete. MMP was low when treated with the electron transport chain inhibitor antimycin, which served as a control (Figure 3.11B). It has long been known that stationary phase yeast have small, round fragmented mitochondria (Westermann, 2012), as seen in WT overnight samples (Figure 3.11B). Notably, the *npr2Δ* cells in stationary phase had more tubular mitochondria, suggesting a defect in fission.

***npr2*Δ Mutants Cannot Activate the Retrograde Response Pathway for Glutamate and Glutamine Synthesis**

I next sought to understand the basis of the inefficient TCA cycle utilization in *npr2*Δ mutants. The expression of several TCA cycle enzymes that were decreased in *npr2*Δ mutants is regulated by the mitochondrial retrograde response transcription factors Rtg1p-Rtg3p. Mitochondrial dysfunction or poor nitrogen sources cause the Rtg1p-Rtg3p transcription factor to translocate into the nucleus and activate genes that are important for adaptation to respiratory deficiency (Butow and Avadhani, 2004). Supplementation with glutamine releases Rtg1p-Rtg3p to the cytoplasm (Butow and Avadhani, 2004). The Rtg1p-Rtg3p target genes include several enzymes of the TCA cycle, such as *CIT1* and *ACO1* (Liu and Butow, 1999). This is because even in the absence of respiration, the first enzymes of the TCA cycle are still required for the synthesis of the non-essential amino acid glutamate, which is derived from the TCA cycle intermediate α -ketoglutarate. Intriguingly, the retrograde response is also regulated by TORC1, as rapamycin induces nuclear translocation of Rtg1p-Rtg3p (Komeili et al., 2000). Due to low amounts of glutamate and glutamine, reduced amounts of TCA cycle enzymes, and dysregulation of TORC1 in *npr2*Δ cells, we suspected that the retrograde response might be defective in such mutants. Consistent with this possibility, *rtg1*Δ mutants have reduced citrate synthase, aconitase and isocitrate dehydrogenase protein and enzyme activities and behave as glutamate and aspartate auxotrophs (Liao and Butow, 1993; Small et al., 1995).

I made an Rtg1-GFP strain with a C-terminal GFP tag to detect the localization of the Rtg1p-Rtg3p transcription factors using fluorescence microscopy. Nic96p was tagged with mCherry to mark the nuclear envelope. In SD medium, WT cells exhibited

nuclear localization of Rtg1-GFP, but the transcription factor remained in the cytosol in *npr2Δ* mutants (Figure 3.12). As expected, the addition of either the electron transport chain complex III inhibitor antimycin or the TORC1 inhibitor rapamycin was sufficient to cause Rtg1-GFP to enter the nucleus in both WT and *npr2Δ* cells (Figure 3.12). In contrast, glutamine as well as aspartate addition was sufficient to cause export of Rtg1-GFP out of the nucleus in WT cells (Figure 3.12). Thus, under minimal glucose conditions, cells normally activate the retrograde response for the synthesis of glutamate and glutamine from the nitrogen source ammonium. In contrast, *npr2Δ* cells appeared tricked into thinking they are aspartate, glutamine, and nitrogen-replete, and do not turn on the retrograde response.

Downstream targets of the Rtg1p-Rtg3p transcription factor, such as *CIT1* and *CIT2*, were measured as another readout of the activity of retrograde pathway. There were significant decreases in *CIT1* and *CIT2* at both the mRNA and protein level in *npr2Δ* cells (Figure 3.13A, B). Taken together, these phenotypes are all indicative of a defective retrograde response in *npr2Δ* cells, and reveal they do not appropriately utilize the mitochondria to boost the synthesis of glutamate, glutamine, and aspartate.

I then asked whether restoration of the retrograde response might improve the growth of *npr2Δ* mutants in SD medium. To restore the retrograde pathway, Mks1p, a kinase that phosphorylates Rtg3p and therefore inhibits the nuclear localization of Rtg1p-Rtg3p (Sekito et al., 2002), was knocked out with the hope of releasing Rtg1p-Rtg3p into the nucleus. However, the kinase is involved in multiple signaling pathways and the knockout strain was too sick for use in such experiments. Next, I attempted to overexpress Rtg2p. Since *rtg2Δ* cells have hyperphosphorylated Rtg3, which inhibits the

retrograde pathway, Rtg2p overexpression should help release the transcription factor into the nucleus (Sekito et al., 2002). However, 3 different constructs to achieve Rtg2p overexpression were unable to rescue the growth of *npr2Δ* cells in SD medium. It is possible that Rtg2p overexpression strains did not result in the intended consequences on the retrograde response due to incorrect expression level, folding etc. However, I then thought about targeting Rtg1p. Although Rtg3p is responsible for the nuclear localization of the Rtg1p-Rtg3p transcription factor, Rtg1p is the key for target gene activation (Sekito et al., 2002).

Therefore, I decided to force the nuclear localization of Rtg1p to constitutively activate the retrograde pathway. I constructed a strain expressing a version of Rtg1-GFP containing a strong SV40 large T antigen nuclear localization signal (NLS) SPKKKRKV (Kalderon et al., 1984) from its endogenous locus. Imaging of these cells in rich YPD medium confirmed that Rtg1-NLS-GFP was constitutively present in the nucleus under conditions that would normally trigger its exclusion (Figure 3.14A). In SD medium, the forced nuclear localization of Rtg1p was able to rescue the growth of *npr2Δ* cells to a similar extent as supplementation of glutamine (Figure 3.14B). Taken together, these findings confirm that the inability to turn on the retrograde response is partially responsible for the poor growth of *npr2Δ* cells in minimal glucose medium in the absence of amino acid supplementation.

***npr2Δ* Mutants Exhibit Compromised Nucleotide Production**

Beyond their functions as amino acids, glutamine and aspartate play additional roles in cellular metabolism and biosynthesis. Glutamine is a nitrogen donor in both de

novo purine and pyrimidine synthesis, while aspartate donates nitrogen for purine synthesis and its carbons for pyrimidine synthesis. Due to the importance of nucleotide metabolism for cell growth and proliferation, I then investigated its regulation by GATOR1/SEACIT. To assess nucleotide metabolism, I first measured the nucleotide metabolites in the cells. With mass spec metabolite analysis, I observed that *npr2Δ*, *npr3Δ* and *iml1Δ* cells contained reduced nucleotide amounts compared to WT (Figure 3.15A). Aspartate supplementation rescued the intracellular levels of nucleotide metabolites in *npr2Δ* cells (Figure 3.15B). The α -ketoglutarate, aspartate, glutamine, and glutamate levels were also rescued to a significant extent by aspartate in *npr2Δ* cells (Figure 3.15C). The overall differences between the metabolomes of WT and *npr2Δ* cells were diminished by aspartate supplementation (Figure 3.15, 3.16), consistent with the complete rescue of growth, further indicating the importance of Npr2p to the regulation of aspartate synthesis in minimal medium. Glutamine or retrograde pathway activation by Rtg1-NLS-GFP did not rescue the nucleotide metabolites to the same extent as aspartate (Figure 3.17), which is consistent with the partial rescue of growth by glutamine or retrograde pathway activation.

To understand the basis of the changes in nucleotide metabolites, I examined the expression of enzymes in the nucleotide synthesis pathway (Figure 3.18A). Analysis of mRNA amounts by qPCR showed that *npr2Δ* cells exhibited reduced mRNA expression of pyrimidine biosynthetic enzymes, including *URA1*, *URA2*, *URA3*, *URA4*, *URA5*, *URA6*, as well as two purine biosynthetic enzymes, *ADE4* (5-phosphoribosyl-1-pyrophosphate amidotransferase), the rate-determining enzyme, and *ADE17* (5-aminoimidazole-4-carboxamide ribonucleotide transformylase) (Figure 3.18B) (Smolina

and Bekker, 1982). Western blot of flag-tagged strains also showed that *npr2Δ* cells had less Ade4p and Ade17p in SD (Figure 3.18C).

Knowing that *npr2Δ* cells had less bulk nucleotide metabolites and less nucleotide biosynthesis enzymes, it is like that *npr2Δ* cells produce less nucleotide metabolites. To measure the synthesis rate of nucleotide metabolites, I employed a LC-MS/MS based ammonium-¹⁵N tracing method. The labeled nucleotide metabolites indeed showed that *npr2Δ* cells produce less nucleotide metabolites (Fig. 3.19). Therefore, the mutants are compromised in their ability to utilize ammonium for the synthesis of the nitrogenous bases present in these nucleotides. Reduced de novo synthesis of nucleotides is consistent with the reduced synthesis of aspartate and glutamine in *npr2Δ* cells.

To assess whether the deficiencies in nucleotide metabolism caused the growth defect of *npr2Δ* mutants, I tested whether supplementation of nucleosides or nitrogenous bases could rescue growth in SD medium. None of the nucleoside or nitrogenous base combinations could improve the growth of *npr2Δ* mutants (Figure 3.20). Therefore, the deficiencies in nucleotide synthesis are not the primary cause of the poor growth. It is likely that additional functions for aspartate and glutamine are important for growth, such as their roles in protein synthesis and other downstream cellular functions. For example, aspartate is also required for asparagine and methionine synthesis, which could explain the partial rescue of growth by these additional amino acids (Figure 3.2). Nonetheless, these findings support a role for TORC1 in promoting the synthesis of glutamine, and especially aspartate, from the TCA cycle for purposes of nucleotide synthesis. Loss of the GATOR1/SEACIT complex deprives cells of the ability to properly regulate the

synthesis of these amino acids from the TCA cycle, and therefore nucleotide synthesis is also compromised.

Genetic Screen for Modifiers of GATOR1/SEACIT Function

To investigate the molecular mechanism of GATOR1/SEACIT, numerous directed genetic manipulations or small metabolite additions were attempted to rescue the growth of *npr2Δ* cells, none of which were successful (table 3.2, table 3.3). To expand this approach, I decided to perform an unbiased genetic screen to look for regulators of Npr2p. *npr2Δ* mutants grew poorly on SD plate at pH 3.4, allowing them to be easily distinguished from WT colonies (Figure 3.21A). Two different plasmid libraries were used for the screen, one with high copy number plasmid (1-2 copies per cell), the other with low copy number plasmid (~50 copies per cell).

A high copy number plasmid library was constructed in the pGP564 plasmid with a 2 micron sequence, *LEU2* marker and yeast genomic fragments. The library was used to rescue *npr2Δ*, *leu2Δ* cells (Figure 3.21B). No significant clones that rescued *npr2Δ* mutants were identified from more than 72,000 transformants, which is > 40 times coverage of the genome. A plasmid with only the *NPR2* gene was constructed and transformed into the *npr2Δ*, *leu2Δ* cells and the transformants still grew poorly on SD-Leu plate at pH 3.4 (Figure 3.21B), perhaps due to overexpression of *NPR2*.

Then I used a low copy number plasmid library containing a *CEN/ARS*, *KANMX4 G418*-resistance marker and yeast genomic fragments (Jauert et al., 2005) to rescue the growth of *npr2Δ* cells on SD plate at pH 3.4 (Figure 3.21C). 10 out of 900,000 transformants had significant rescue of *npr2Δ* mutants on SD-G418 plate. Sequencing of the plasmids revealed that they were all from the same clone containing *CIT1*, *AVT2*,

CAN1 and *NPR2* (Figure 3.21C). Overexpression of each individual gene in *npr2Δ* cells showed that *NPR2* was the only gene identified in the screen to rescue the growth defect of *npr2Δ* cells.

Summary

Since its original discovery in budding yeast in 1991, the regulation of TORC1 signaling has been closely linked to the quality of nitrogen sources (Beck and Hall, 1999; Komeili et al., 2000; MacGurn et al., 2011; Merhi and Andre, 2012). While yeasts can utilize a variety of nitrogenous compounds to synthesize all essential nitrogen-containing metabolites, glutamine is their most favorable nitrogen source (Godard et al., 2007). When given less preferred nitrogen sources, yeast cells activate Gln3p, the transcriptional activator of nitrogen catabolite repressed (NCR) genes, to enable their assimilation to glutamine (Rai et al., 2015). This is largely achieved through inhibition of TORC1-mediated phosphorylation of Gln3p, which promotes its nuclear localization (Beck and Hall, 1999). In addition to Gln3p, yeast cells are also dependent on the Rtg1p/Rtg3p transcription factors for the synthesis of glutamine (Butow and Avadhani, 2004). Since both rapamycin and mitochondrial dysfunction lead to nuclear translocation of Rtg1p/Rtg3p and induction of the mitochondrial retrograde response, the cellular response to either amino acid starvation or respiratory deficiency involves induction of a gene expression program geared towards the synthesis of glutamate and glutamine (Butow and Avadhani, 2004). Under such conditions, cells are expected to decrease glutamine consumption and instead focus on its preservation. Consistent with this idea, we previously observed that amino acid starvation induced autophagy leads cells to

accumulate glutamine (Laxman et al., 2014). In contrast, during growth, glutamine is consumed rapidly due to its requirement as a nitrogen donor for the biosynthesis of nitrogen-containing metabolites such as nucleotides (Laxman et al., 2014).

The GATOR1/SEACIT complex is a conserved negative regulator of TORC1 that functions in response to amino acid availability (Kim et al., 2008; Panchaud et al., 2013). Through analysis and rescue of the slow growth phenotype of *npr2Δ* mutants growing under high glucose, amino acid starved conditions, I showed that a fundamental metabolic function of TORC1 is to promote the synthesis and utilization of the amino acids aspartate and glutamine, which are derived from cataplerotic reactions of the mitochondrial TCA cycle, in response to nitrogen quality and the availability of the preferred nitrogen source (Fig. 3.22). Indeed, *npr2Δ* mutants have hyperphosphorylated Gln3p and a defective retrograde response even under glutamine deficiency. Although these pathways are clearly responsive to glutamine, how glutamine is sensed in cells to elicit the proper regulation of these transcription factors remains an open question (Duran et al., 2012; Jewell et al., 2015; Nicklin et al., 2009; Stracka et al., 2014). It might not be sensed directly, as *npr2Δ* cells have increased TORC1 signaling and proliferative metabolism despite substantially lower absolute amounts of intracellular glutamine as a result of its rapid consumption for biosynthesis during growth (Laxman et al., 2014). Moreover, there is a discrepancy between the phosphorylation status of Sch9p, the most commonly used readout of TORC1 in yeast, and other TORC1 activity markers. In such high glucose conditions, *npr2Δ* cells have hyperphosphorylated Gln3p and Npr1p, yet exhibit reduced Sch9p phosphorylation and reduced phospho-S6. It has been proposed that the AGC kinase Ypk3p, rather than Sch9p, might be the true yeast ortholog of S6K

(Gonzalez et al., 2015). However, the fact that the *npr2Δ* mutant exhibits a rapamycin-reversible, slow growth phenotype just as a GTP-locked *GTR1* Q65L mutant suggests they in fact have hyperactive TORC1 signaling. Thus, the primary role of TORC1 activity may be the regulation of metabolism, which normally positively affects cell growth. Sch9p phosphorylation status may be more directly correlated with cell growth and proliferation than TORC1 activity. Nonetheless, our findings suggest caution must be used when correlating the phosphorylation status of TORC1 substrates with the growth and amino acid status of cells.

Despite the importance of glutamine, aspartate may in fact be a more critical and demanding output of TORC1. Notably, despite the many alterations in transcription, protein levels, and phosphorylation status of metabolic enzymes caused by loss of Npr2p, the sole addition of aspartate was sufficient to completely rescue the growth of *npr2Δ* mutant cells. My study showed that TORC1 utilizes mitochondrial TCA cycle activity for the purpose of aspartate synthesis rather than for ATP, as the growth of *npr2Δ* cells with low TCA cycle activity can be completely rescued by adding modest concentrations of aspartate (Figure 3.2B). Aspartate, like glutamine, is also involved in protein, purine and pyrimidine synthesis. However, the supplementation of various combinations of nucleosides and nucleobases was unable to rescue the growth of *npr2Δ* cells, suggesting that the effects of aspartate and glutamine extend beyond just nucleotide synthesis. It is notable that aspartate synthesis from oxaloacetate requires glutamate as the nitrogen donor. Glutamate synthesis from α -ketoglutarate consumes NAD(P)H, while aspartate synthesis would be impaired by high NADH due to the reversibility of malate dehydrogenase and depletion of oxaloacetate to malate (Figure 3.7). Thus, aspartate

synthesis would be dependent on glutamate availability as well as a more proper NAD⁺/NADH ratio (Figure 3.9A), perhaps explaining why *npr2Δ* cells with mitochondrial dysfunction might be more dependent on aspartate than glutamine. Aspartate is also needed for the synthesis of asparagine, methionine, and arginine.

Several recent studies proposed a major function of mitochondrial respiration in mammalian cells is to support aspartate synthesis (Birsoy et al., 2015; Cardaci et al., 2015; Sullivan et al., 2015). The exact mechanism of mitochondrial regulation by TORC1 is unclear. Physical interaction between GATOR1/SEACIT (figure 2.1C, table 2.1) (Algret et al., 2014) and the fact that Npr2p is also found in vCLAMP (mitochondrial-vacuole patch) (Elbaz-Alon et al., 2014) hint that they may communicate through mitochondrial-vacuole organelle contacts and perhaps small metabolite exchange. Pyruvate was suggested to function as an electron acceptor to support aspartate synthesis and growth in the absence of a functional electron transport chain. However, pyruvate supplementation alone and other attempts to boost the NAD⁺/NADH ratio thus far could not rescue the growth of *npr2Δ* mutant yeast cells (Figure 3.9B). The defect in aspartate synthesis in *npr2Δ* cells is not just due to a redox issue, but stems from a collective set of impairments due to dysregulated TORC1 signaling. TORC1 through its kinase activity exerts its effects via a variety of transcriptional, translational, and post-translational mechanisms to rewire cellular metabolism in a manner to promote aspartate synthesis, in addition to glutamine. The impact is so broad that manipulating single gene or pathway is not sufficient to rescue the defect (Table 3.2, 3.3), but so specific that simple supplementation of aspartate can reverse the phenotype. Furthermore, in mammalian cells, mTORC1 was reported to stimulate both purine and pyrimidine synthesis (Ben-Sahra et

al., 2013; Ben-Sahra et al., 2016). Here I showed that the ability of mTORC1 to promote nucleotide synthesis is likely a consequence of its activation of glutamine and aspartate synthesis. Moreover, the metabolic functions of TORC1 extend beyond just nucleotide synthesis, but to other important metabolites important for proliferative growth, such as NAD⁺ and glutathione, with their common link being dependency on these nitrogenous amino acids (Laxman et al., 2014). It follows that activation of aspartate and glutamine synthesis can impact numerous additional downstream processes, such as protein translation and ribosome biogenesis, which are dependent on increased nucleotide synthesis for rRNA transcription.

Taken together, my findings point to a specific metabolic function for inhibitors of TORC1 signaling such as GATOR1/SEACIT – that is to regulate key cataplerotic reactions of the mitochondrial TCA cycle in tune with the amino acid and nitrogen status of cells (Figure 3.22). It is not a coincidence that aspartate and glutamine are in essence nitrogenous forms of the TCA cycle intermediates oxaloacetate and α -ketoglutarate. While TORC1 activation promotes such cataplerotic reactions and their subsequent use for biosynthesis to support proliferative metabolism, TORC1 inhibition promotes anaplerotic reactions that aim to restore TCA cycle intermediates to ensure that the TCA cycle can be utilized for ATP synthesis under starvation or stress conditions. Consistent with this idea, the majority of transcriptional targets of the retrograde response, which is activated upon inhibition of TORC1 signaling, promote anaplerotic reactions that function to replenish TCA cycle intermediates (Butow and Avadhani, 2004; Komeili et al., 2000). Properly balancing these disparate TCA cycle functions is likely to be intrinsically important throughout the life of a cell, and loss of this capability might be

especially detrimental under nutritional or metabolic stress. Lastly, the findings reported here might offer an additional explanation for the metabolic basis of aerobic glycolysis and the Warburg effect that is often observed in rapidly proliferating cell types: if the mitochondrial TCA cycle intermediates α -ketoglutarate and oxaloacetate must be consumed for the synthesis of glutamine and aspartate to support biosynthetic demands, then cells have no choice but to become less reliant on the TCA cycle and respiration for ATP generation.

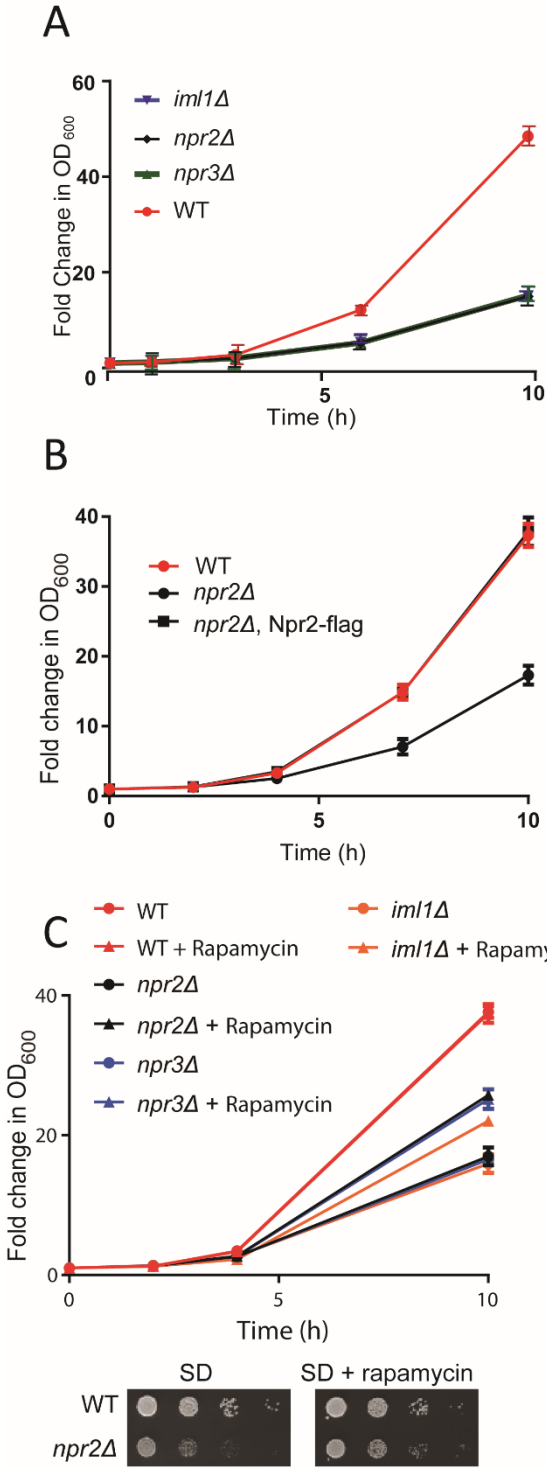


Figure 3.1 *npr2*Δ growth defect in SD medium is caused by high TORC activity

A) Growth of wild type (WT), *iml1*Δ, *npr2*Δ, and *npr3*Δ strains in minimal medium with glucose (SD) that lacks any supplemented amino acids. Data were mean +/- STD from 3 independent experiments. The phenotypes of *iml1*Δ, *npr2*Δ, and *npr3*Δ have been identical in all tested conditions thus far.

B) Growth curves of WT, *npr2*Δ and *npr2*Δ, Npr2-flag (*npr2*Δ with reintroduction of Npr2-flag) in SD. Data were collected from 2 independent experiments.

C) Growth curves of WT, *npr2*Δ, *npr3*Δ and *iml1*Δ in SD supplemented with 2 nM rapamycin (upper). Data were collected from 2 independent experiments (upper). Serial dilution of cells (WT, *npr2*Δ) were spotted onto agar plates (10,000, 1,000, 100, 10 cells for each spot) and incubated at 30°C for 2 days (lower). Growth media were SD (left) or SD with 1 nM rapamycin.

D) Serial dilution of cells (WT, *npr2*Δ, *gtr1*Δ, *npr2gtr1*Δ and GTR1 Q65L-flag) were spotted as described in B. Growth media were YPD (left) or SD (right). GTR1 Q65L-Flag is a GTP-locked mutant of Gtr1p (Nakashima et al., 1999).

E) Western blots depicting Gln3p, Sch9p, Npr1p and phospho-S6 proteoforms in WT and *npr2*Δ cells switched from YPD to SD medium for the indicated times. The Sch9 protein is cleaved by NTCB treatment to observe the mobility shift of the C-terminal peptide. 200 ng/mL rapamycin or 25 μg/mL cycloheximide was added as controls for inhibition or stimulation of TORC1 signaling. G6PDH serves as the loading control.

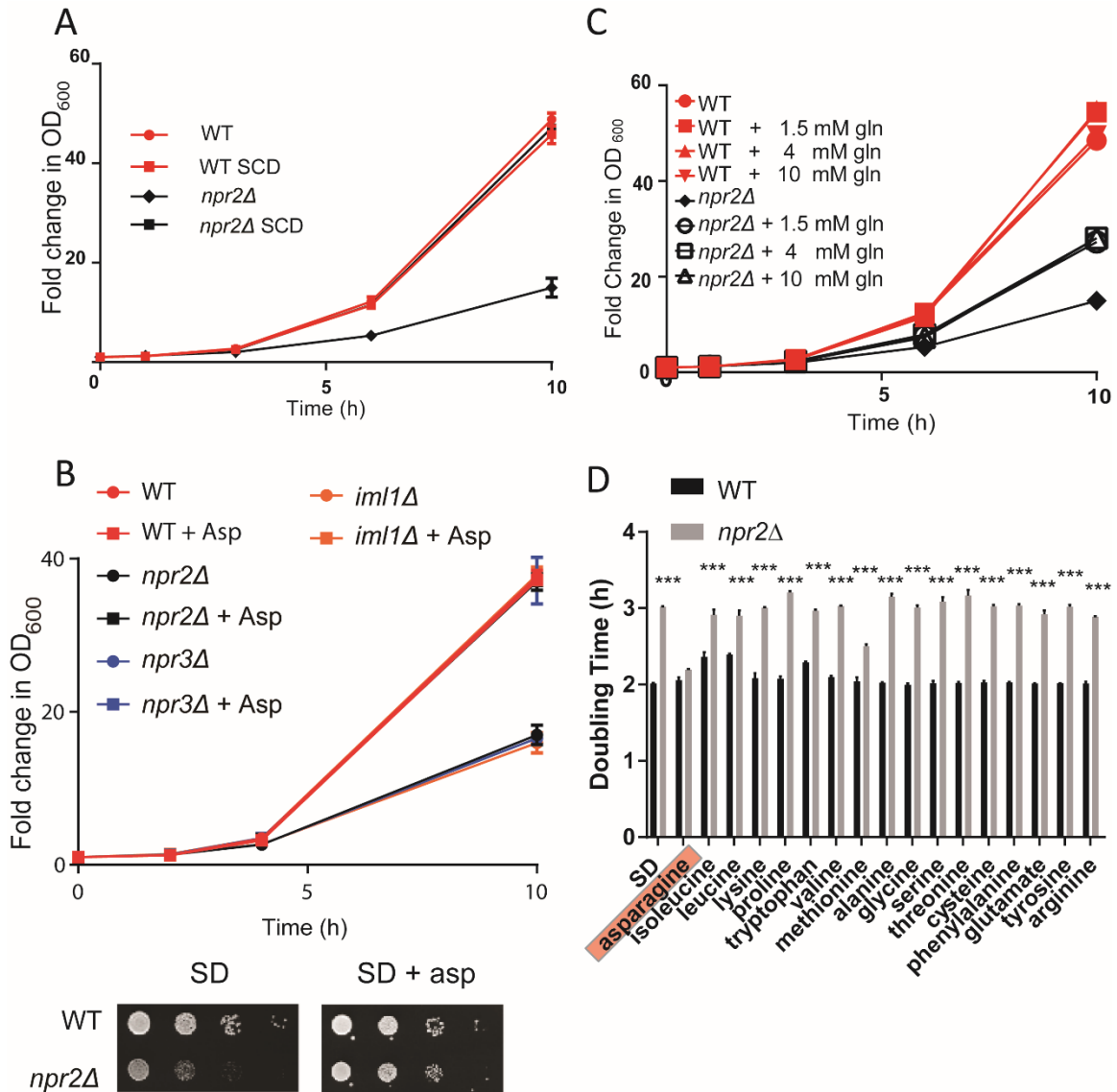


Figure 3.2 *npr2Δ* growth defect in SD can be completely rescued by aspartate or partially by glutamine

A) Growth curves of WT and *npr2Δ* in either SD or SCD (supplemented with complete supplement mixture which contains amino acids mixture). Data were collected from 2 independent experiments.

B) Growth curves of WT, *npr2Δ*, *npr3Δ* and *iml1Δ* in SD supplemented with 2 mM aspartate. Data were collected from 2 independent experiments (upper). Serial dilutions of cells (WT, *npr2Δ*) were spotted onto agar plates of SD (left) or SD with 2 mM aspartate (lower).

C) Growth of WT or *npr2Δ* cells with or without supplementation of indicated amounts of glutamine. Data were mean +/- STD from 3 independent experiments.

D) Doubling time of WT and *npr2Δ* cells in SD medium supplemented with 2 mM of the indicated amino acids (tyrosine was added to 1 mM due to low solubility). Asparagine can completely rescue the growth of *npr2Δ* cells (highlighted in orange). Data were mean +/- STD from 3 independent experiments. ****p* < 0.001 by two-tailed Student's t-test.

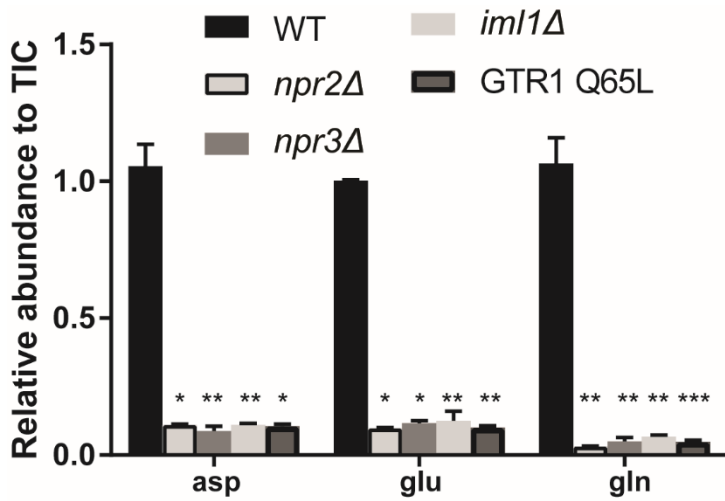


Figure 3.3 Relative abundance of intracellular glutamine, glutamate and aspartate in WT, *npr2*Δ, *npr3*Δ, *iml1*Δ and GTR1 Q65L cells quantitated by LC-MS/MS.

Yeast cells were collected after switch from YPD to SD for 6 hours and extracted for metabolites. Data were mean +/- STD from 2 independent experiments with duplicates. * $p < 0.05$, ** $p < 0.01$, *** $p < 0.001$ by two-tailed Student's t-test.

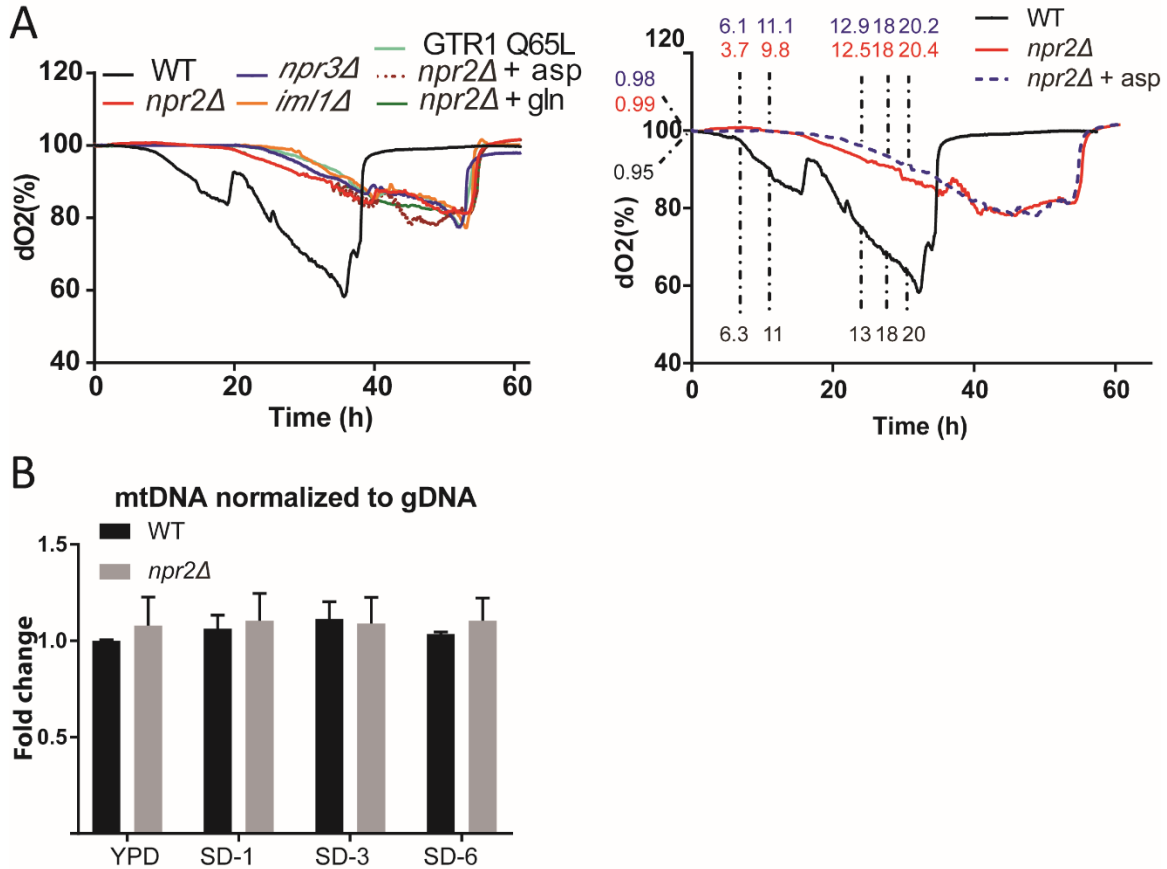


Figure 3.4 *npr2Δ* cells have defective mitochondria

A) Dissolved oxygen levels as a function of growth following inoculation into SD medium. WT, *npr2Δ*, *npr3Δ*, *iml1Δ*, and GTR1 Q65L strains were grown in parallel bioreactor vessels, and the *npr2Δ* strains were also supplemented with 2 mM aspartate or glutamine (left). On the right panel, the OD₆₀₀ readings of corresponding time points were labeled on the dissolved oxygen traces for WT (black), *npr2Δ* (red), and *npr2Δ* supplemented with 5 mM aspartate (blue). Representative data were selected from 2 independent experiments.

B) Mitochondrial DNA content in WT and *npr2Δ* cells following switch from YPD to SD for a period of 1, 3, 6 h. Data were mean +/- STD from 2 independent experiments.

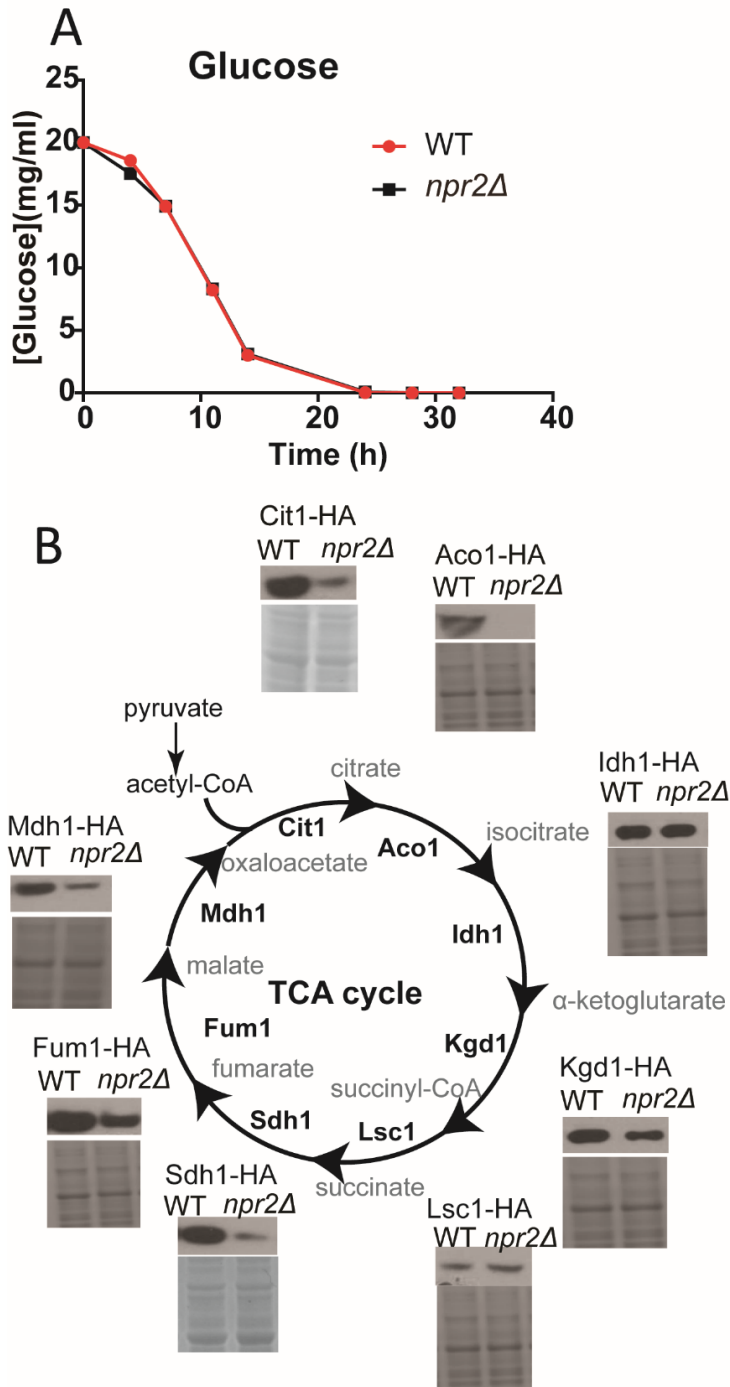


Figure 3.5: *npr2Δ* cells express less mitochondrial TCA cycle enzymes

A) Glucose concentration in the medium over time in SD.

B) Western blots indicating amounts of HA-tagged TCA cycle enzymes: Aco1p (aconitase), Cit1p (citrate synthase), Idh1p (isocitrate dehydrogenase), Kgd1p (α -ketoglutarate dehydrogenase), Lsc1p (succinyl-CoA ligase), Sdh1p (succinate dehydrogenase), Fum1p (fumarase) and Mdh1p (mitochondrial malate dehydrogenase) in WT and *npr2Δ* cells grown in SD for 6 hours. Total protein level (Coomassie blue stain) is shown as loading control.

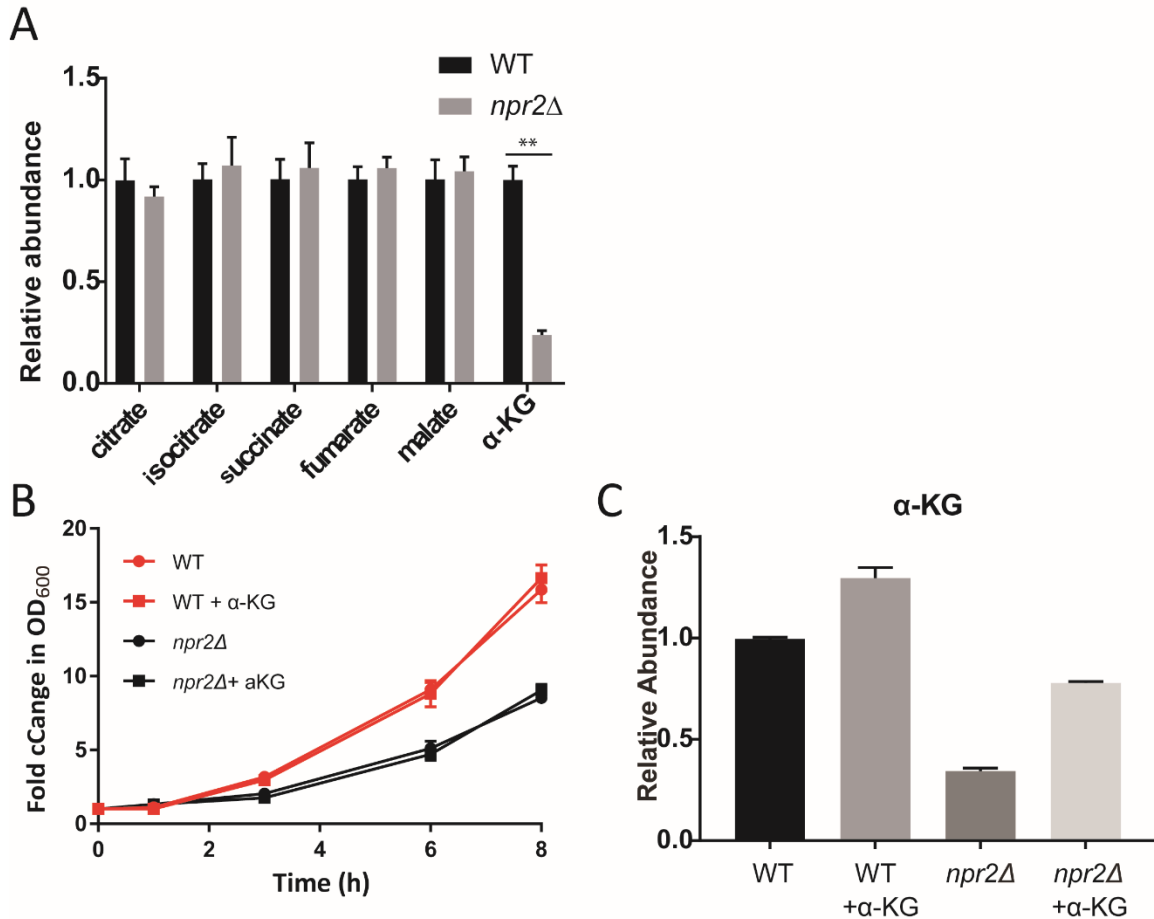


Figure 3.6: *npr2Δ* cells have lower TCA cycle activity

A) TCA cycle metabolite levels were quantitated by LC-MS/MS. Cells were collected after switch from YPD to SD for 6 h. Data were mean \pm STD from 3 independent experiments. $**p < 0.01$ by two-tailed Student's t test.

B) Growth rate of WT and *npr2Δ* cells in SD with or without 2 mM dimethyl 2-oxoglutarate (membrane permeable α -KG, labeled as α -KG). Data were mean \pm STD from 2 independent experiments.

C) α -ketoglutarate levels were quantitated by LC-MS/MS. Cells were collected after switch from YPD to SD or SD supplemented with 2 mM dimethyl 2-oxoglutarate (membrane permeable α -KG, labeled as α -KG) for 6 h. Data were mean \pm STD from 2 independent experiments. $**p < 0.01$ by two-tailed Student's t test.

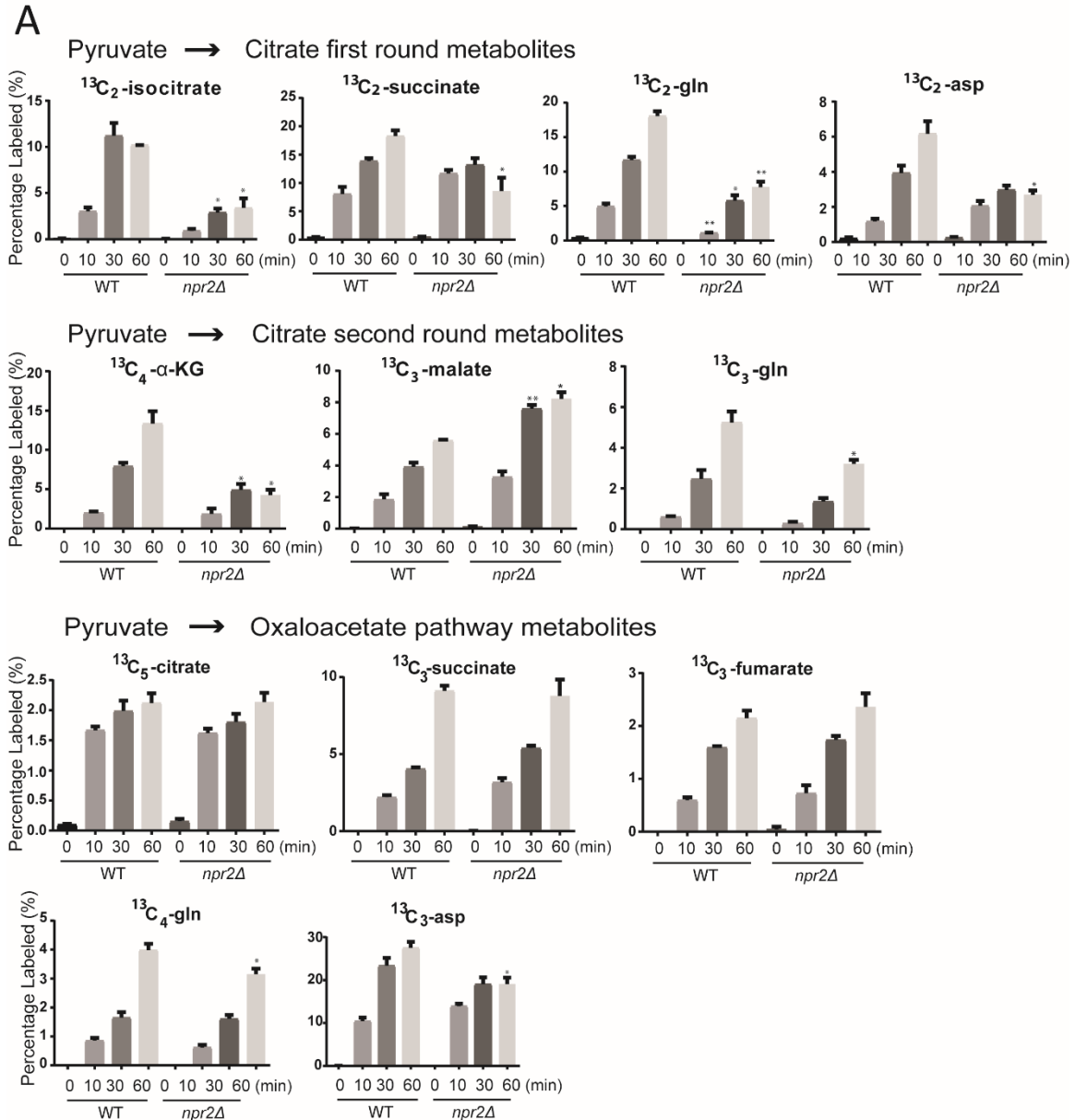


Figure 3.7: Relative abundance of labeled TCA cycle metabolites from glucose- $^{13}\text{C}_6$ tracing experiments.

Labeled species are shown as percentage of all isotopomers of the respective metabolite. Glucose- $^{13}\text{C}_6$ is converted into pyruvate. Pyruvate can be converted into acetyl-CoA, and all first round TCA cycle metabolites are M+2 labeled. The final product M+2 oxaloacetate in combination with M+2 labeled acetyl-CoA can give rise to second round metabolites. Pyruvate can also be converted into M+3 oxaloacetate and the TCA products are labeled as listed in Table 3.1. Data were mean \pm STD from 3 independent experiments. * $p < 0.05$, ** $p < 0.01$, *** $p < 0.001$, by two-tailed Student's t-test.

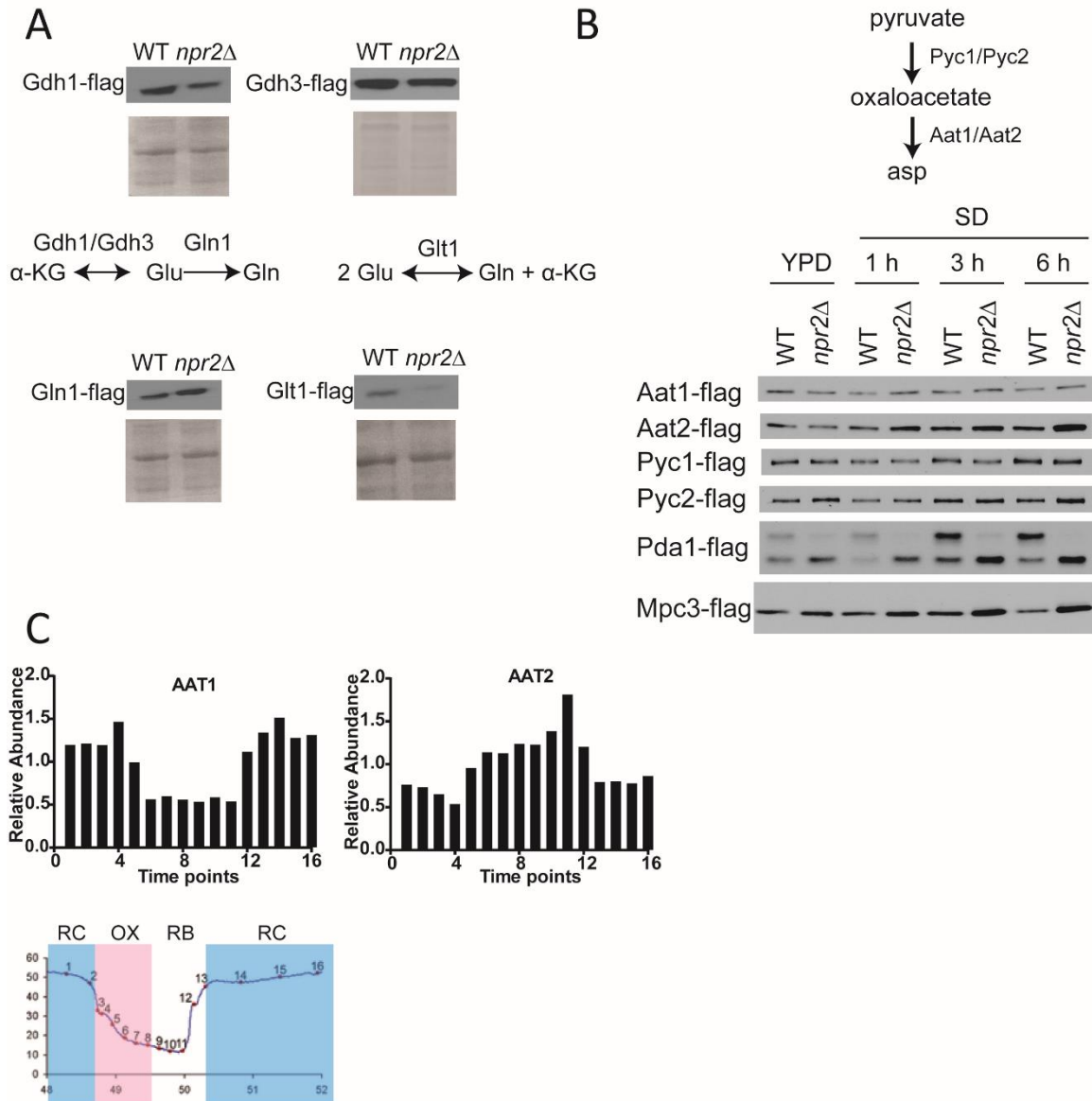


Figure 3.8: *npr2Δ* mutants exhibited hallmarks of oxidative metabolism

A) Western blots indicating amounts of Gdh1p (NADP⁺-dependent glutamate dehydrogenase), Gdh3p (Gdh1p paralog), Glt1p (NAD⁺ - dependent glutamate synthase) and Gln1p (glutamine synthetase) in WT and *npr2Δ* cells collected after switch from YPD to SD for 6 h.

B) Western blots indicating amounts of Aat1p/Aat2p (aspartate aminotransferase), Pyc1p/Pyc2p (pyruvate carboxylase), Pda1p (E1 α subunit of pyruvate dehydrogenase complex), and Mpc3p (mitochondrial pyruvate carrier) in WT and *npr2Δ* cells collected following switch from YPD to SD for 1, 3, 6 h. The Pda1 samples were run on phostag gels with 25 μ M of Phos-TagTM AAL-107 (NARD institute, Ltd.).

C) mRNA expression amounts for AAT1 and AAT2 across 16 time points in the yeast metabolic cycle (YMC). Data are from (Kuang et al., 2014). Note that both AAT1 and AAT2 have expression peaks in either RC or RB phase which are correlated with stress response or mitochondria, as opposed to growth (OX).

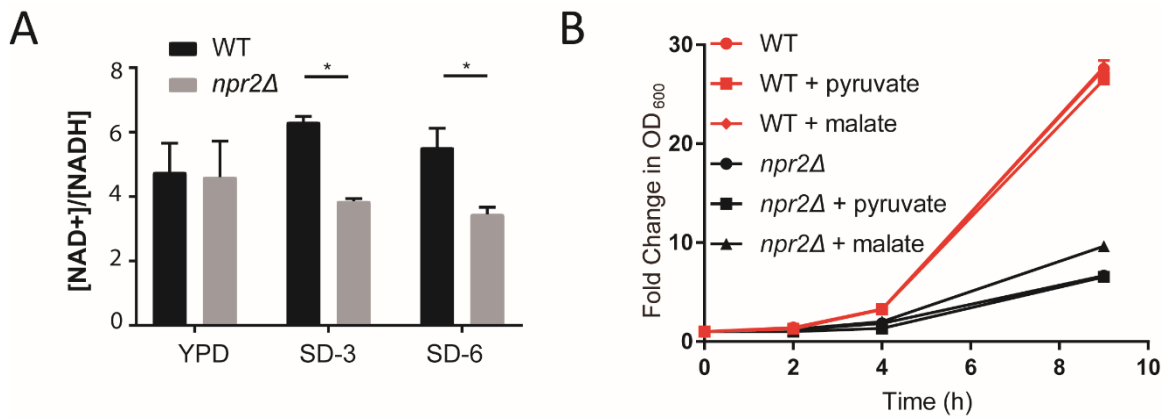


Figure 3.9: *npr2Δ* cells have skewed redox state

A) Intracellular NAD⁺/NADH ratio in YPD or after switch to SD for 3 or 6 h. Data were mean +/- STD from 2 independent experiments. *p < 0.05 by two-tailed Student's t test.

B) Growth rate of WT and *npr2Δ* cells in SD with or without 2 mM dimethyl 2-oxoglutarate (membrane permeable α -KG, labeled as α -KG). Data were mean +/- STD from 2 independent experiments.

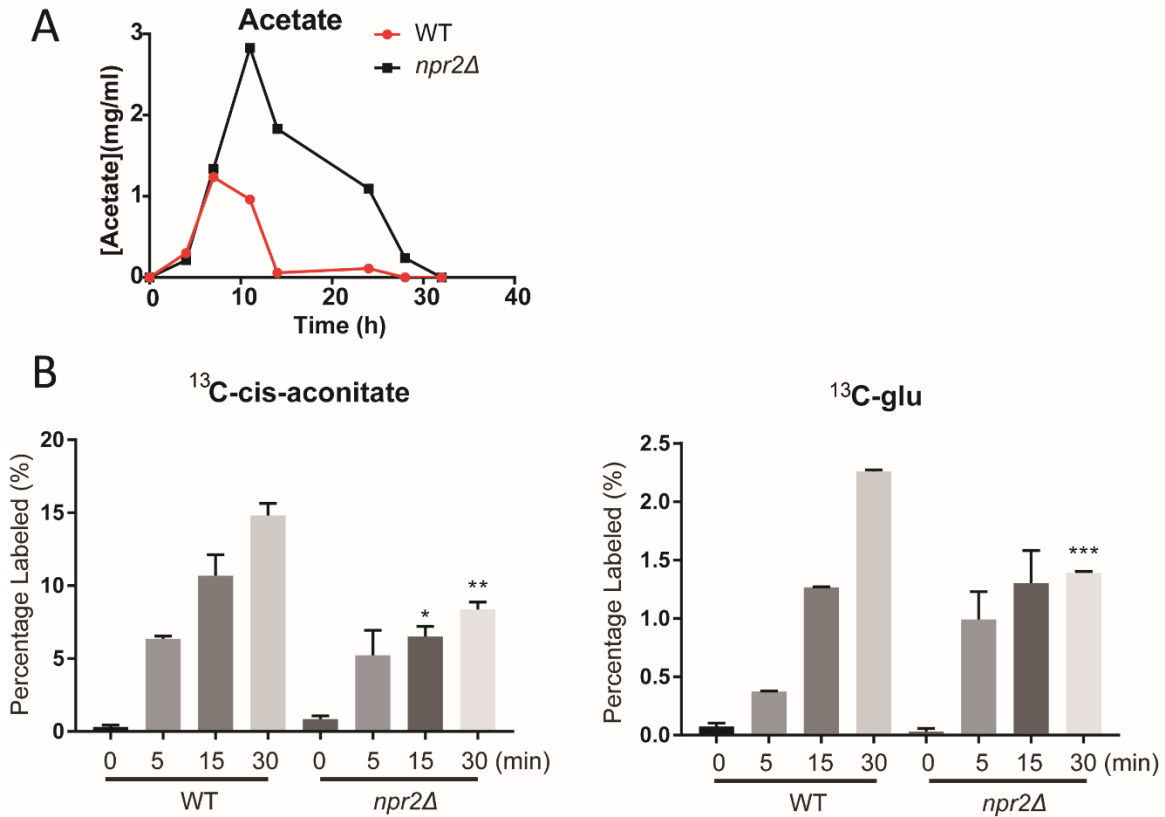


Figure 3.10: *npr2Δ* cells have defect in acetate utilization

A) Acetate concentration in the medium over time in SD.

B) Relative abundance of the labeled cis-aconitate and glutamate from acetate-¹³C₂ tracing experiments. acetate-¹³C₂ is converted into acetyl-CoA which enters the TCA cycle (all M+1 labeled). M+1 α - ketoglutarate from the cycle can be made into M+1 glutamate and M+1 glutamine. The method could detect M+1 cis-aconitate (intermediate between citrate and isocitrate) and M+1 glutamate effectively. Labeled species are shown as percentage of all isotopomers of the respective metabolite. *p < 0.05, **p < 0.01, ***p < 0.001, by two-tailed Student's t test.

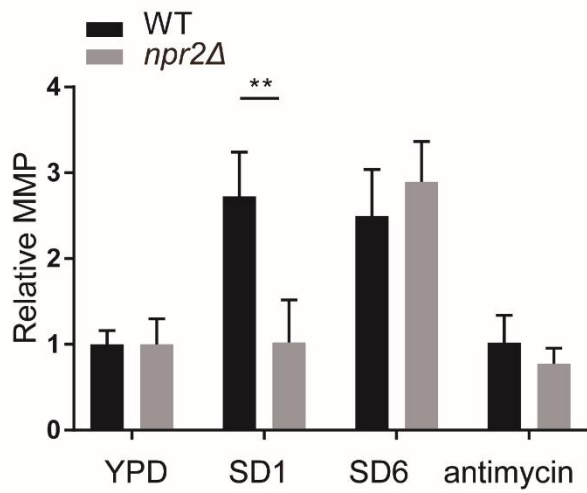
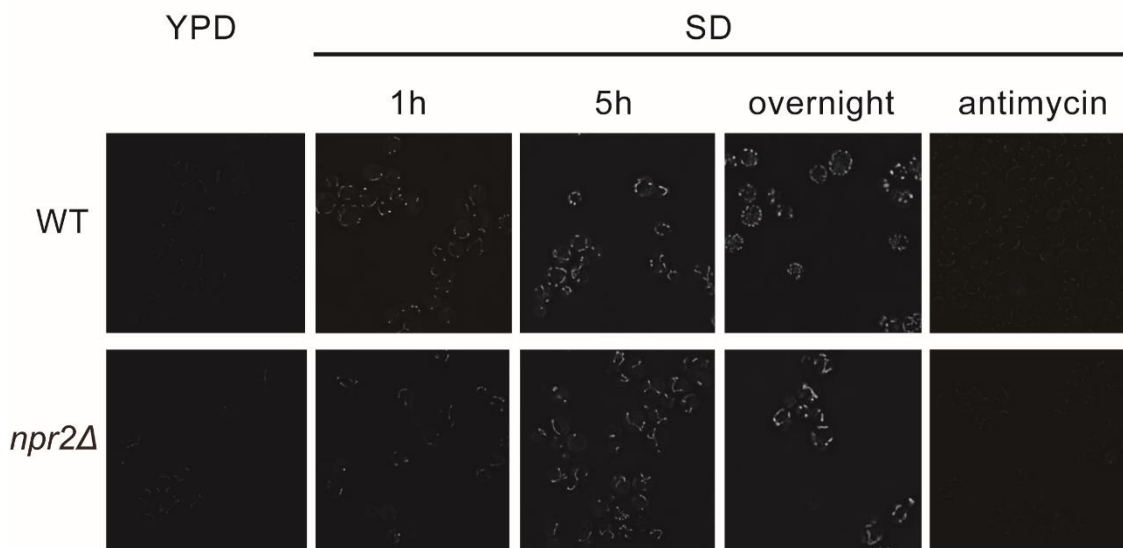
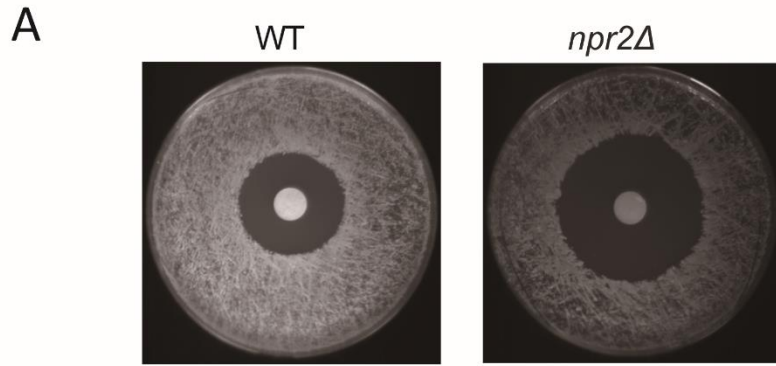


Figure 3.11: *npr2Δ* cells are more susceptible to reactive oxygen species (ROS) stress and have defective mitochondrial membrane potential (MMP) regulation

A) H₂O₂ halo assay for WT and *npr2Δ* cells on SD plate. 0.1 OD of cells were spread onto SD plate. Filter paper discs soaked with 1 M H₂O₂ were placed onto the middle of the plate. The plates were left to grow for 2 days at 30 °C.

B) Mitochondrial membrane potential (MMP) of WT and *npr2Δ* cells upon switch from YPD to SD. Dioc6 (3,3'-dihexyloxacarboyanine iodide) was used to stain for the mitochondria. Antimycin was used as control. The MitoMap plugin in ImageJ was used to assess the mitochondrial network volume, and MitoLoc was used to calculate the MMP intensity (Vowinckel et al., 2015). The relative MMP was shown in the bar graph. The MMP for overnight culture was not calculated as the signal was above the threshold.

Data were mean +/- STD from 2 independent experiments. **p < 0.01 by two-tailed Student's t test.

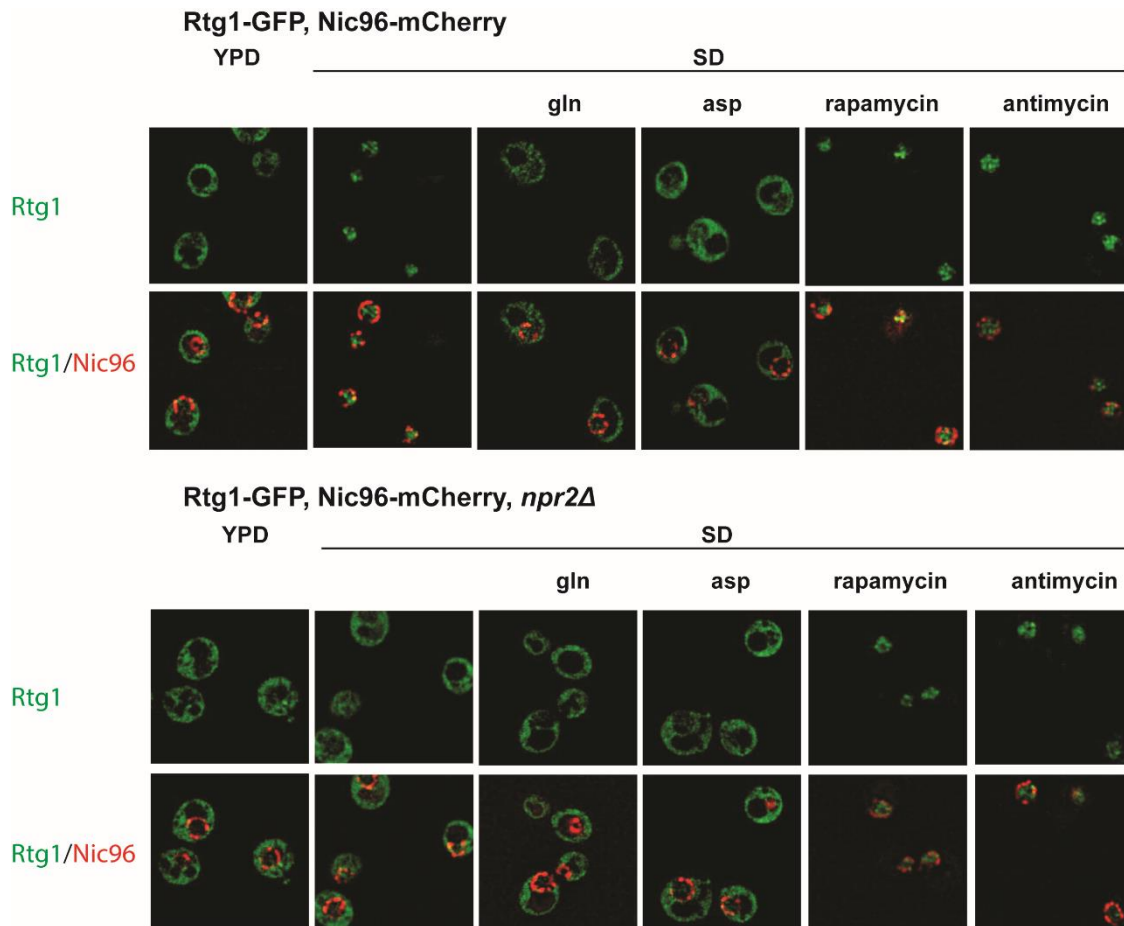


Figure 3.12: *npr2Δ* mutants exhibit a defective mitochondria-to-nucleus retrograde response.

WT or *npr2Δ* cells expressing Rtg1-GFP, Nic96-mCherry (nuclear pore complex marker) were transferred from YPD to SD for 6 hours and treated with mock, 50 μ M antimycin, 50 nM rapamycin, 2 mM glutamine or 2 mM aspartate (pH 5.1) for 30 minutes prior to imaging. Note that *npr2Δ* mutants failed to activate the response and localize Rtg1-GFP to the nucleus following switch to SD medium. Antimycin and rapamycin treatment activated the retrograde response by in both strains, while glutamine or aspartate addition inactivated the pathway in WT cells.

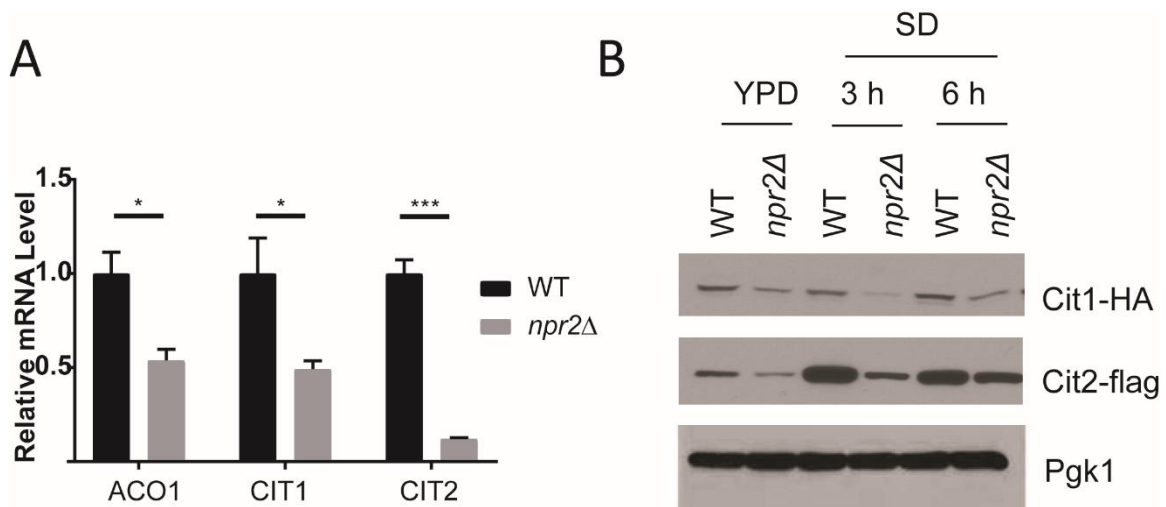


Figure 3.13: *npr2Δ* mutants exhibit a defective retrograde response.

A) mRNA amounts of transcriptional targets of the retrograde response (RTG) pathway, ACO1, CIT1 and CIT2 in WT and *npr2Δ* cells collected following growth in SD for 6 h. Data were mean \pm STD from two independent experiments. * $p < 0.05$, *** $p < 0.001$, by two-tailed Student's t-test.

B) Western blot depicting amounts of retrograde response targets Cit1p and Cit2p in WT and *npr2Δ* cells switched from YPD to SD for indicated times. Note that *npr2Δ* mutants have consistently lower amounts of these enzymes in SD medium.

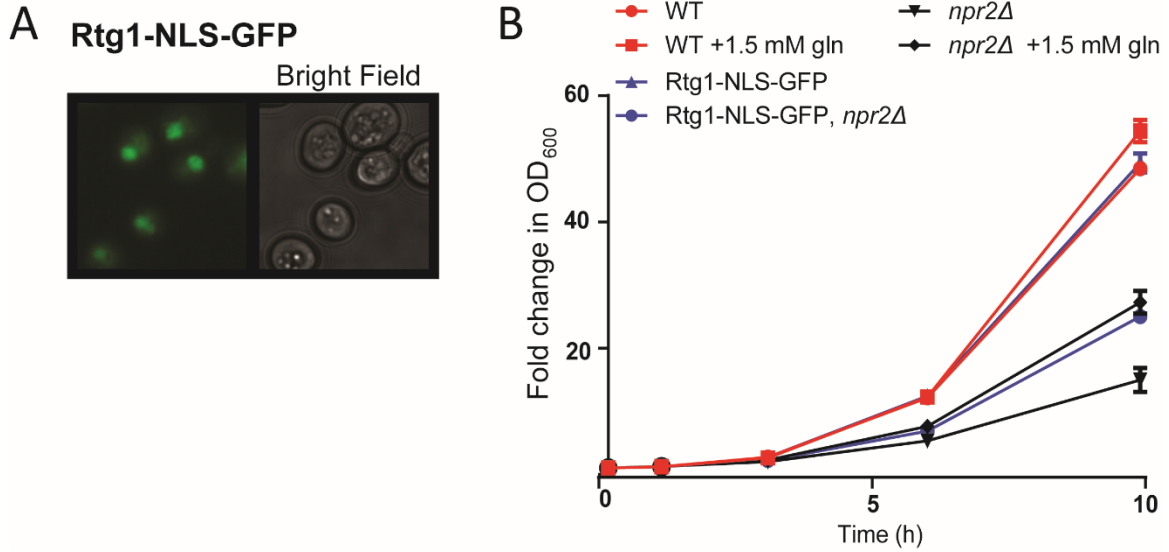
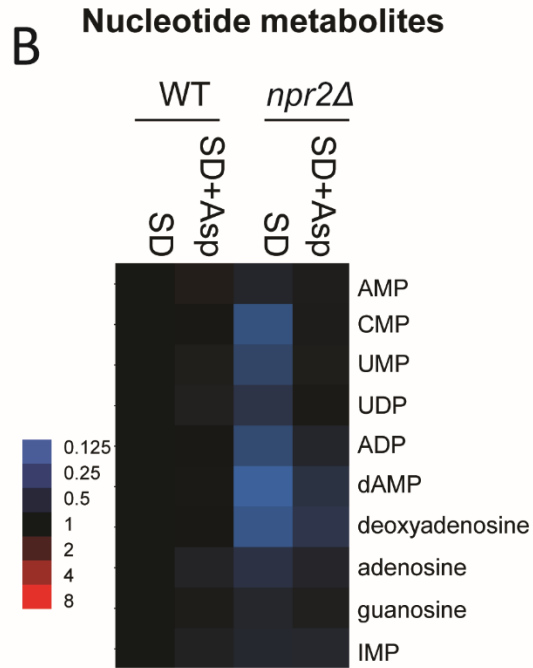
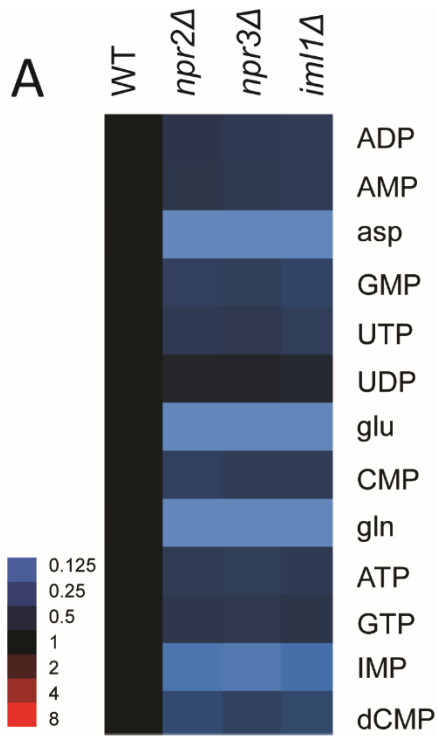


Figure 3.14: Forced nuclear localization of Rtg1p can partially rescue the growth of *npr2Δ* mutants

A) Images of cells expressing Rtg1-NLS-GFP showing the forced nuclear localization of Rtg1p in cells growing in YPD medium.

B) Growth of WT or *npr2Δ* cells expressing a version of Rtg1-GFP containing a strong nuclear localization signal (NLS) (Rtg1-NLS-GFP). Two duplicates at each time point were measured, in two independent experiments.



C
TCA cycle metabolites
and amino acids

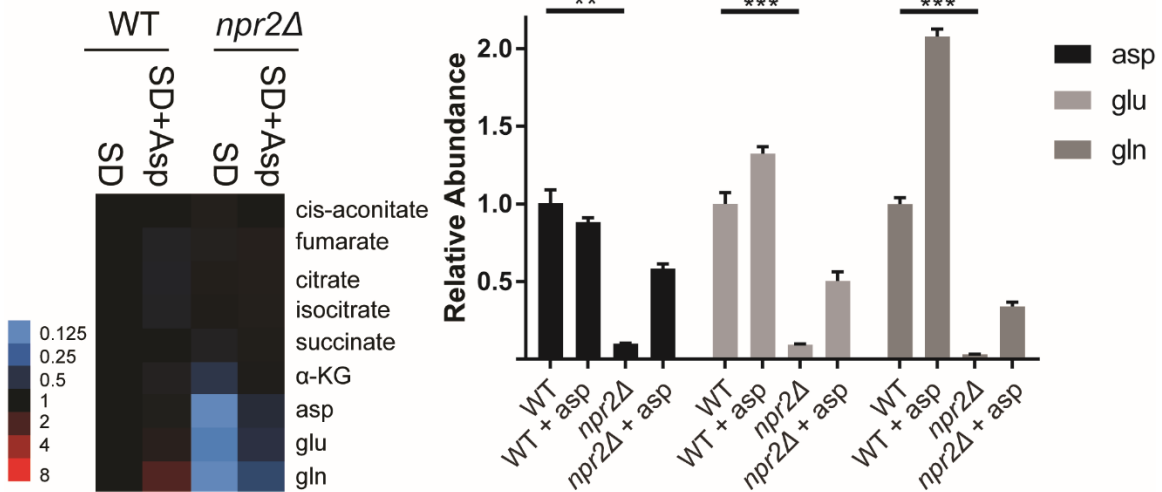


Figure 3.15: Low levels of nucleotide metabolites in *npr2*Δ mutants can be rescued by aspartate

A) Heat map depicting abundance of nucleotide metabolites in WT, *npr2*Δ, *npr3*Δ and *iml1*Δ cells. The aspartate, glutamate and glutamine levels are also specifically shown in bar graph format. Cells were grown in YPD and then transferred into SD for 6 h prior to extraction of metabolites. Intracellular nucleotide metabolites levels were measured with targeted LC-MS/MS methods. Data were collected from 3 independent experiments.

B) Heat map of relative abundance of nucleotide metabolites following aspartate supplementation, normalized against WT. Cells were switched into SD for 6 h as in (A), but with or without addition of 2 mM aspartate. Data were collected from 2 independent experiments. Data were collected from 3 independent experiments.

C) Heat map of relative abundance of TCA cycle metabolites following aspartate supplementation, normalized against WT (Left). Aspartate, glutamate and glutamine levels are also shown in bar graph format (right). Data were mean +/- STD from 3 independent experiments. *p < 0.05, **p < 0.01, ***p < 0.001 by two-tailed Student's t-test.

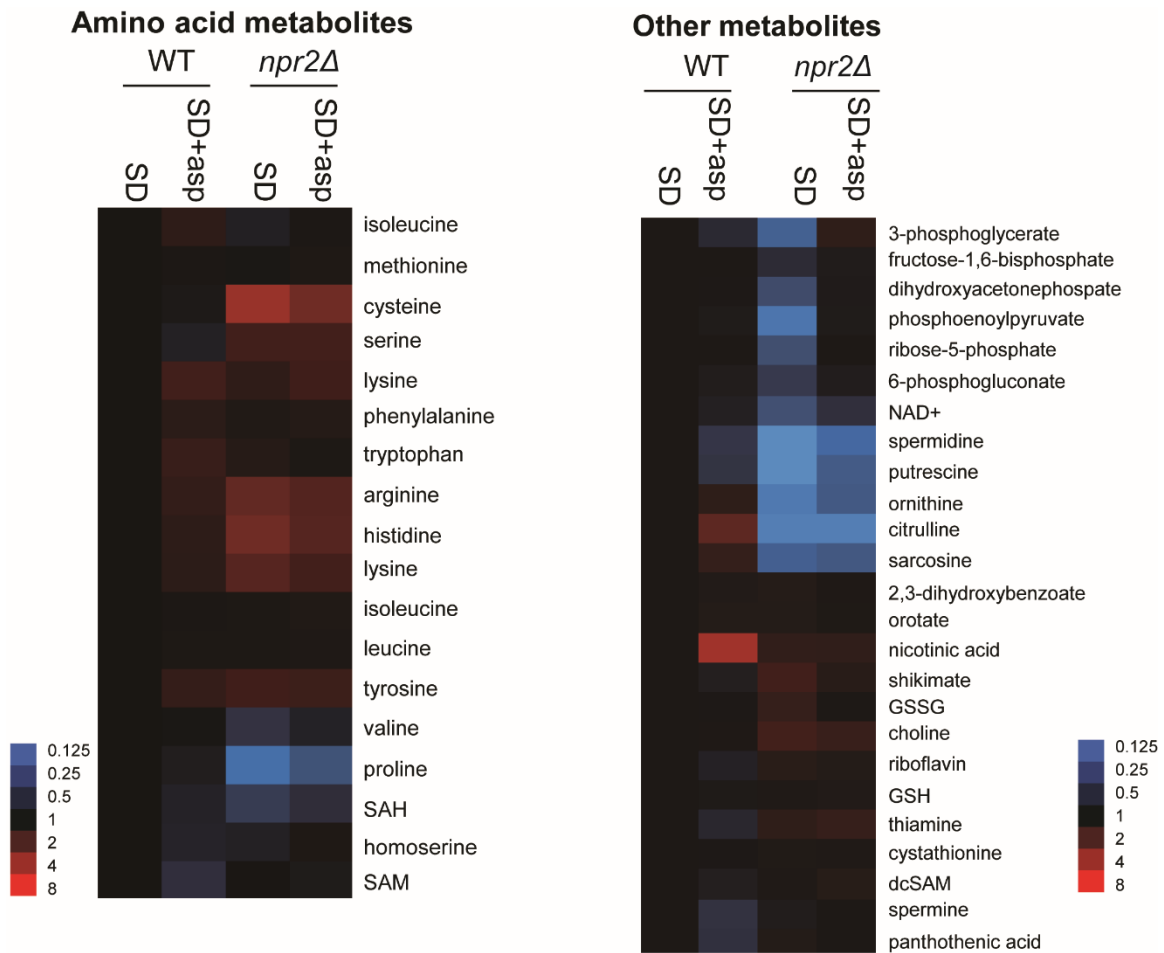


Figure 3.16: Aspartate supplementation rescues the metabolome of *npr2Δ* mutants
 Heat maps depicting abundances of the indicated metabolites obtained by LC-MS/MS analyses of WT or *npr2Δ* cells grown to OD = 1, in SD or SD supplemented with 2 mM aspartate. Data were collected from 3 independent experiments.

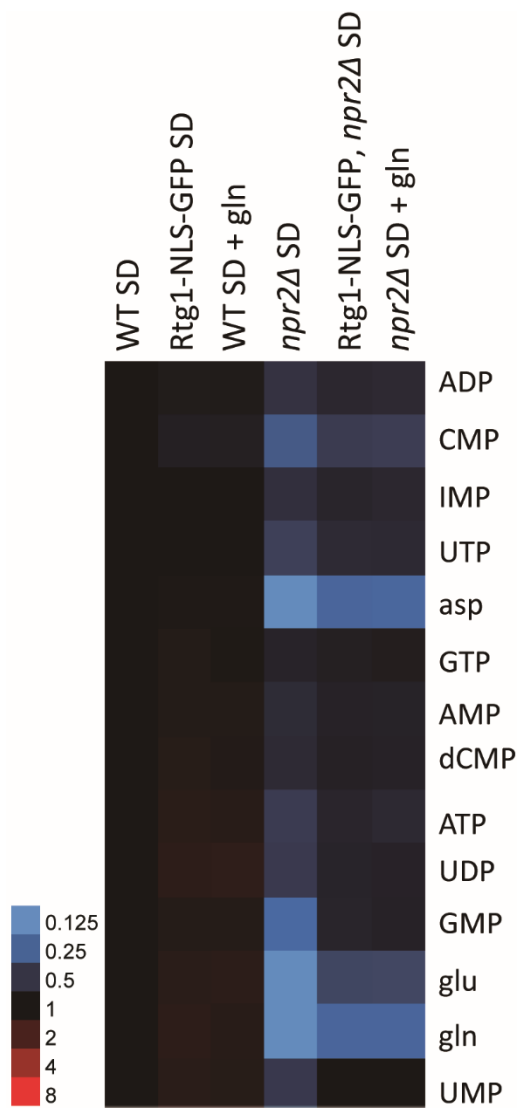


Figure 3.17: Glutamine or retrograde pathway activation does not rescue the nucleotide metabolites of *npr2Δ* mutants

Heat map depicting abundances of the indicated metabolites obtained by LC-MS/MS analyses of WT or *npr2Δ* or Rtg1-NLS-GFP cells switched from YPD to SD with or without 2 mM glutamine for 6 h. Data were collected from 2 independent experiments.

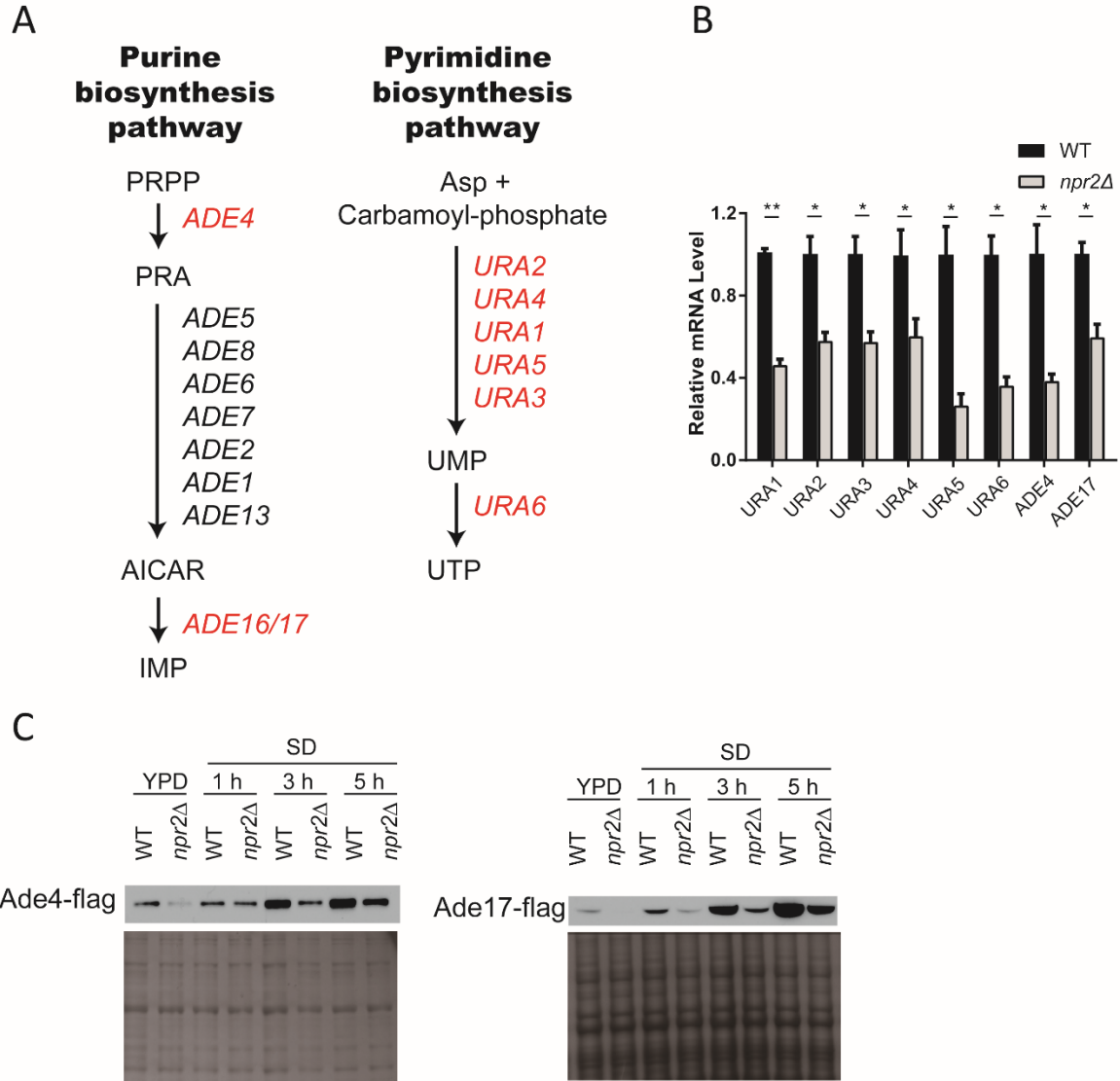


Figure 3.18: *npr2Δ* cells express less nucleotide biosynthesis pathway enzymes

A) de novo biosynthesis pathway of purine and pyrimidine nucleotides.

B) mRNA levels of pyrimidine synthesis pathway enzymes (URA1, URA2, URA3, URA4, URA5, URA6) and purine synthesis pathway (ADE4, ADE17) from WT and *npr2Δ* cells. Cells were grown in YPD and then transferred into SD for 6 hours before collection. Data were mean \pm STD from 2 independent experiments with duplicates for each genotype. * $p < 0.05$, ** $p < 0.01$, by two-tailed Student's t-test.

C) Western blot depicting amounts of retrograde response targets Cit1p and Cit2p in WT and *npr2Δ* cells switched from YPD to SD for indicated times. Note that *npr2Δ* mutants have consistently lower amounts of these enzymes in SD medium.

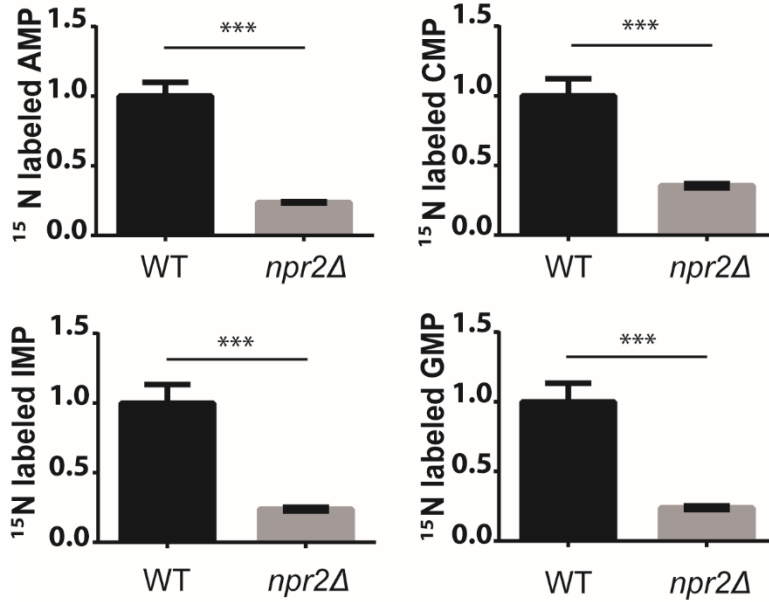


Figure 3.19: *npr2Δ* cells have a lower rate of nucleotide metabolite synthesis

Relative abundance of labeled nucleotide metabolites from [¹⁵N]-ammonium tracing experiments. Cells were grown in YPD and then transferred into SD for 3 h, and then switched into SD-N plus 5 g/L ammonium-¹⁵N₂ sulfate for 1 h. Data were mean +/- STD from 3 independent experiments. ***p<0.001, by two-tailed Student's t-test.

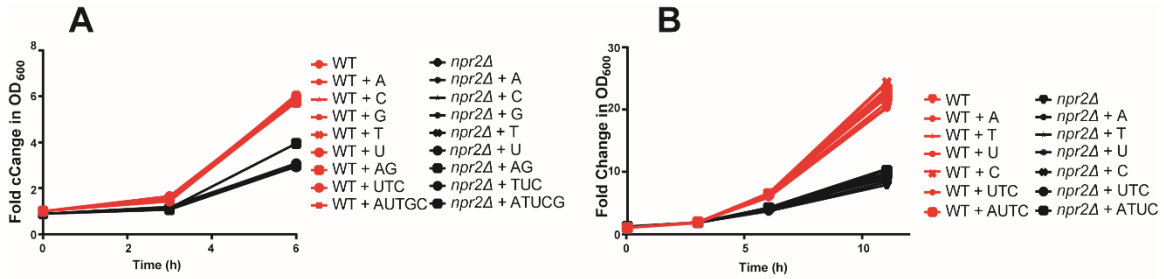


Figure 3.20: The slow growth of *npr2Δ* cells cannot be rescued by nucleoside or nucleobase plus ribose supplementation

A) Growth of WT and *npr2Δ* cells in SD supplemented with different combinations of nucleosides at 20 mg/L. A (adenosine), C (cytidine), G (guanosine), T (thymidine), U (uridine), AG (adenosine and guanosine, all purine nucleosides), UTC (uridine, thymidine, cytidine, all pyrimidine nucleosides), AUTCG (all nucleosides). Data were mean +/- STD from 2 independent experiments.

B) Growth of WT and *npr2Δ* cells in SD supplemented with different combinations of nucleobases at 20 mg/L, with 5 mM of ribose. A (adenine), C (cytosine), T (thymine), U (uracil), UTC (uracil, thymine, cytosine, all pyrimidine nucleobases), AUTC (all nucleobases). Guanine is poorly soluble in water and not supplemented in the experiments. Data were mean +/- STD from 2 independent experiments.

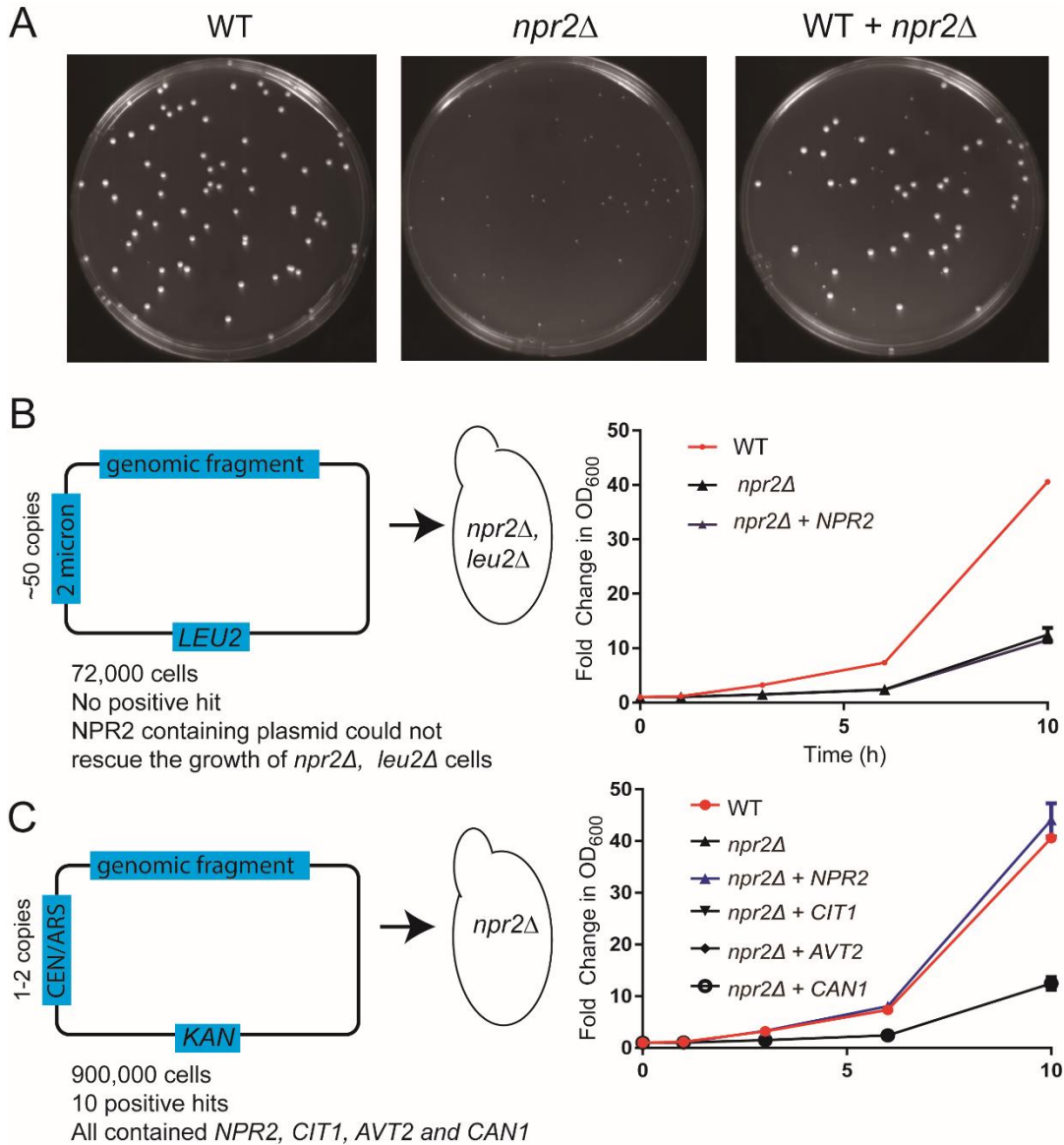


Figure 3.21: Genetic screen for Npr2p regulators

A) Growth of colonies arise from single cell of WT or *npr2Δ* cells on SD plate at pH 3.4.

B) The high copy suppressor screen is based on a high copy plasmid with 2 micron, LEU2 marker. *npr2Δ*, *leu2Δ* cells were transformed with the library in YPD medium, washed and screened for regulators that could rescue the growth on SD plate at pH 3.4. There was no positive hit from the screen, even the positive control – NPR2 gene containing high copy plasmid did not rescue the growth of *npr2Δ*, *leu2Δ* cells.

C) The low copy suppressor screen is based on a low copy plasmid with CEN/ARS, KANMX4 G418-resistant selectable marker. *npr2Δ* cells were transformed with the library in YPD medium, washed and screened for regulators that could rescue the growth on SD + Kan plate at pH 3.4. There were 10 positive hits from the screen, all containing a genomic fragment with *NPR2*, *CIT1*, *AVT2*, and *CAN1*. Individual genes were cloned into low copy plasmid and expressed in the *npr2Δ* background to measure the growth. Only the *NPR2* expression (in blue) rescued the growth.

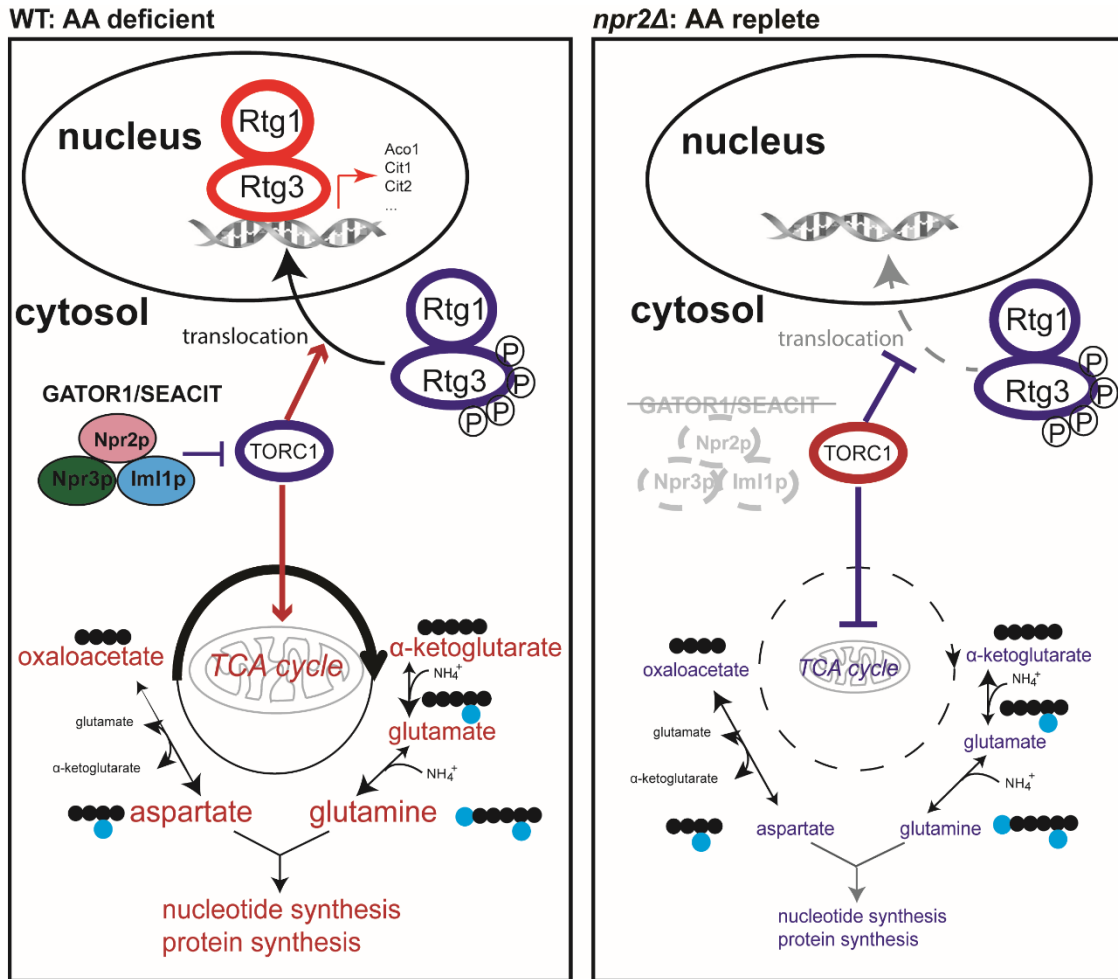


Figure 3.22: Npr2p and GATOR1/SEACIT regulate cataplerotic reactions of the mitochondrial TCA cycle in tune with the amino acid and nitrogen status of cells.

In glucose medium, yeast cells preferentially perform glycolysis and reduce TCA cycle activity. When starved for amino acids (SD medium), WT cells are able to sense the lack of amino acids and regulate TORC1 activity through Npr2p and the GATOR1/SEACIT complex. As a result, WT cells boost TCA cycle activity as well as the retrograde response pathway for the production of glutamine and aspartate from α -ketoglutarate and oxaloacetate (cataplerotic reactions), which are consumed to make these nitrogen-containing amino acids. In *npr2Δ* mutants, the cells perceive themselves to be amino acid-replete. Hyperactive TORC1 inhibits the replenishment of α -ketoglutarate and oxaloacetate due to dysregulation of the retrograde response pathway and metabolic reactions that feed the TCA cycle (anaplerotic reactions). Cells exhaust the TCA cycle intermediate pool, further inhibiting TCA cycle functions and resulting in crisis. Thus, the GATOR1/SEACIT complex regulates TORC1 activity to balance cataplerotic and anaplerotic reactions of the TCA cycle in tune with the amino acid and nitrogen status of cells. Red denotes activation, blue denotes inhibition.

Table 3.1: List of labeled TCA metabolites, glutamine, and aspartate from glucose-¹³C₆ tracing experiments by LC-MS/MS

¹³ C ₃ Pyruvate ¹³ C ₂ Acetyl-CoA				
Name	MW	¹³ C MW	Q1/Q3 <i>m/z</i> (neg. mode)	
¹³ C ₂ -Isocitrate	192	194	193/75	
¹³ C ₂ -Succinate	118	120	119/75	
¹³ C ₂ -Glutamine	146	148	147/129	
¹³ C ₂ -Aspartate	133	135	134/117	
2nd round metabolites				
¹³ C ₄ - α -ketoglutarate	145	149	148/104	
¹³ C ₃ -Malate	134	137	136/118	
¹³ C ₃ -Glutamine	146	149	148/112	
¹³ C ₃ Pyruvate ¹³ C ₃ Oxaloacetate				
¹³ C ₅ -Citrate	192	197	196/111	
¹³ C ₃ -Succinate	118	121	120/75	
¹³ C ₃ -Fumarate	116	119	118/73	
¹³ C ₃ -Aspartate	133	136	135/118	
¹³ C ₄ -Glutamine	146	150	149/131	

Table 3.2: Genetic manipulation attempts to rescue slow growth of *npr2Δ* cells

Genotype	Gene function	Phenotype
Knockouts		
<i>pda1Δ</i>	Pyruvate dehydrogenase	No effect
<i>pkp1Δ</i>	Mitochondrial protein kinase	No effect
<i>pkp2Δ</i>	Mitochondrial protein kinase	No effect
<i>ptc5Δ</i>	Mitochondrial type 2C protein phosphatase	No effect
<i>ptc6Δ</i>	Mitochondrial type 2C protein phosphatase	No effect
<i>pck1Δ</i>	Phosphoenolpyruvate carboxykinase	No effect
<i>reg1Δ</i>	Regulatory subunit of type 1 protein phosphatase Glc7p;	Synthetic lethal in <i>npr2Δ</i>
<i>mdh3Δ</i>	Peroxisomal malate dehydrogenase	No effect
<i>mdh2Δ</i>	Cytoplasmic malate dehydrogenase	No effect
<i>mdh1Δ</i>	Mitochondrial malate dehydrogenase	No effect
<i>mpc2Δ</i>	Mitochondrial pyruvate carrier	No effect
<i>mpc3Δ</i>	Mitochondrial pyruvate carrier	No effect
<i>aat1Δ</i>	Mitochondrial aspartate aminotransferase	No effect
<i>aat2Δ</i>	Cytosolic aspartate aminotransferase	Severe growth defect
<i>aat1Δ ,aat2Δ</i>		Severe growth defect
<i>bat1Δ</i>	Mitochondrial branched-chain amino acid aminotransferase	No effect
<i>bat2Δ</i>	Cytosolic branched-chain amino acid (BCAA) aminotransferase	No effect
<i>bat1Δ, bat2Δ</i>		Severe growth defect
<i>avt4Δ</i>	Vacuolar transporter for large neutral amino acids	No effect
<i>avt6Δ</i>	Vacuolar aspartate and glutamate exporter	No effect
<i>fau1Δ</i>	5,10-methenyltetrahydrofolate synthetase	No effect
<i>ade16Δ</i>	Enzyme of 'de novo' purine biosynthesis	No effect
<i>ade17Δ</i>	Enzyme of 'de novo' purine biosynthesis	No effect
<i>cit2Δ</i>	Peroxisomal citrate synthase	No effect
<i>acs1Δ</i>	Acetyl-CoA synthetase	No effect
<i>mls1Δ</i>	Malate synthase	No effect
<i>gad1Δ</i>	Glutamate decarboxylase	No effect
<i>idp2Δ</i>	Cytosolic NADP-specific isocitrate dehydrogenase	No effect
<i>icl1Δ</i>	Isocitrate lyase	No effect
<i>sfc1Δ</i>	Mitochondrial succinate-fumarate transporter	No effect
<i>dic1Δ</i>	Mitochondrial dicarboxylate carrier	No effect
<i>mks1Δ</i>	Negative regulator of the RTG pathway	Severe growth defect
<i>ssy1Δ</i>	SPS plasma membrane amino acid sensor system	No effect
<i>gcn4Δ</i>	bZIP transcriptional activator of amino acid biosynthetic genes in response to amino acid starvation	Slight growth defect
<i>dld1Δ</i>	Major mitochondrial D-lactate dehydrogenase	No effect
<i>dld2Δ</i>	2-hydroxyglutarate dehydrogenase, and minor D-lactate	No effect

	dehydrogenase	
<i>dld3Δ</i>	2-hydroxyglutarate transhydrogenase, and minor D-lactate dehydrogenase	No effect
<i>cyb2Δ</i>	L-lactate cytochrome-c oxidoreductase	No effect
<i>ppm1Δ</i>	Carboxyl methyltransferase	Severe growth defect
<i>shm2Δ</i>	Cytosolic serine hydroxymethyltransferase	KO makes WT grow like <i>npr2Δ</i> on plate
<i>pho2Δ</i>	Homeobox transcription factor involved in regulating basal and induced expression of genes of the purine and histidine biosynthesis pathways	KO makes WT grow like <i>npr2Δ</i> on plate
<i>bas1Δ</i>	Myb-related transcription factor involved in regulating basal and induced expression of genes of the purine and histidine biosynthesis pathways	KO makes WT grow like <i>npr2Δ</i> on plate
<i>akr1Δ</i>	Palmitoyl transferase	KO rescues <i>npr2Δ</i> growth on plate but has major morphology issues
<i>pyc1Δ</i>	Pyruvate carboxylase	Severe growth defect
<i>pyc2Δ</i>	Pyruvate carboxylase	No effect
<i>pyc1Δ, pyc2Δ</i>		Severe growth defect
Overexpressions		
Shm2	Cytosolic serine hydroxymethyltransferase	No effect
Idp1	Mitochondrial NADP-specific isocitrate dehydrogenase	No effect
Idp2	Cytosolic NADP-specific isocitrate dehydrogenase	No effect
Idp3	Peroxisomal NADP-dependent isocitrate dehydrogenase	No effect
Ndi1	NADH:ubiquinone oxidoreductase	No effect
Acs1	Acetyl-coA synthetase	No effect
Dld3	2-hydroxyglutarate transhydrogenase, and minor D-lactate dehydrogenase	No effect
Yef1	ATP-NADH kinase	No effect
Utr1	ATP-NADH kinase	No effect
Pos5	Mitochondrial NADH kinase	No effect
Bmh1	14-3-3 protein	No effect
Cit2	Peroxisomal citrate synthase	No effect
Ure2	Nitrogen catabolite repression transcriptional regulator	Severe growth defect
Hap4	Transcription factor for respiratory gene expression	No effect
A.niger PYC	Pyruvate carboxylase from <i>Aspergillus niger</i>	No effect
A.niger PYC, <i>pyc1Δ</i>	Pyruvate carboxylase from <i>Aspergillus niger</i>	Severe growth defect
A.niger PYC, <i>pyc1Δ</i>	Pyruvate carboxylase from <i>Aspergillus niger</i>	No effect
A.niger PYC, <i>pyc1Δ, pyc1Δ</i>	Pyruvate carboxylase from <i>Aspergillus niger</i>	Severe growth defect

Table 3.3: small metabolite rescue attempts for *npr2*Δ cells

Condition	Phenotype
Sodium pyruvate w/o glu, gln, asp	WT has a slight growth defect
Malate w/o glu, gln, asp	No effect
Octyl-ketoglutarate w/o nucleotide/nucleoside combinations	No effect
Nucleotide/nucleoside combinations w/o glu, gln	No effect

CHAPTER FOUR

MATERIAL AND METHODS

Yeast Strains, Gene Deletion and Tagging

The prototrophic CEN.PK strain background was used in all experiments unless specified. Gene deletions or tagging was performed using a PCR-based strategy, by gene replacement using KanR/NatR/HygroR cassettes via homologous recombination (Longtine et al., 1998). Rich medium YPD contained 1% yeast extract, 2% peptone and 2% glucose; YPL contained 1% yeast extract, 2% peptone and 2% lactate; SCD contained 6.7 g/L yeast nitrogen base, ammonium sulfate without amino acids (DIFCO), complete plus 2% glucose; amino acid starved SD medium contains 6.7 g/L yeast nitrogen base, ammonium sulfate without amino acids (DIFCO), plus 2% glucose; SL contained 6.7 g/L yeast nitrogen base, ammonium sulfate without amino acids (DIFCO), plus 2% lactate. Complete supplement mixture (CSM) were purchased from Sunrise Science Products and QBiogene. Amino acids, nucleotides, nucleosides and riboses were purchased from Sigma-Aldrich, made into stock solution and stored at -20 °C before use. For the second part of the thesis, unless specified, cells were grown in YPD overnight and then switched to YPD and SD. Cell growth curves were typically initiated at OD₆₀₀ ~ 0.1.

Yeast Metabolic Cycle

The yeast metabolic cycle was established using chemostats as previously described (Tu et al., 2005). 10 ml of overnight culture of Npr2-flag or WT cells were inoculated into 1 L fermenter vessel. When the metabolic cycles stabilized after starvation and continuous feeding, 50 -100 OD cells were collected at various phases, spun down and snap frozen in liquid nitrogen and stored at -80 °C.

Flag Tagged Protein Immunoprecipitation

Cells were grown to log phase or collected at desired time points and stored at -80 °C. Invitrogen Dynabeads TM protein G (Thermo Fisher Scientific) were pre-cleared with BSA and then incubated with monoclonal anti-flag M2 antibody (Sigma) and lysis buffer (100 mM NaCl, 50 mM NaF, 100 mM Tris-HCl pH 7.5, 1 mM EDTA, 1 mM EGTA, 0.1% Tween 20, 10% glycerol, 100 mM sodium orthovanadate, protease inhibitor (Roche), 100 mM PMSF, 5 μM pepstatin, 10 μM leupeptin, 14 mM β-mercaptoethanol) at room temperature for 20 minutes. The cells were lysed with pre-chilled lysis buffer with bead beater. The lysate was mixed with anti-flag antibody conjugated beads and rotated at 4 °C for 1 hour. The beads were washed with ice cold lysis buffer and mixed with 3XFlag peptide. The eluted supernatant was mixed with 2X sample loading buffer (100 mM Tris-HCl, pH 6.8, 4% SDS, 20% glycerol, 200 mM DTT, 0.2% bromophenol blue) and resolved on SDS-PAGE gel.

Silver Stain

Silver stain of SDS-PAGE gel was performed with the Pierce Silver Stain Kit (Thermo Fisher Scientific). The gel was washed with ultrapure water, fixed with fixing solution (30% ethanol, 10% acetic acid, 60% water), then washed with 10% ethanol then water. Afterwards, the gel was sensitized with Sensitizer from the kit, washed and stained with Stain Working solution for 30 minutes. Then develop with Developer Working Solution until the bands were visible and had good contrast. The staining reaction was stopped with stop solution (5% acetic acid) then washed and stored in water.

Mass Spectrometry Protein Identification

The silver stained gel was cut with new blade on glass board into desired size with extra care to avoid human contamination. The bands were stored in sterile Eppendorf tube at 4°C and sent to Proteomic Core facility for trypsin digestion and mass spectrometry protein identification.

Protein Co-immunoprecipitation

The cell lysis and pull-down procedure were the same with flag-tagged protein immunoprecipitation. 3XFlag peptide elution was not performed. The Dyna Beads were boiled with 2 X sample loading buffer and loaded to SDS-PAGE gel for western blotting.

DNA/RNA Purifications and RT-qPCR

RNA was isolated with the MasterPure Yeast RNA kit (Epicentre). Reverse transcription was performed on 1 µg of purified RNA, using SuperScript II reverse transcriptase (Invitrogen). Quantitative PCR was performed using SYBR Green (Bio-Rad), primers, and template cDNA. Transcript abundance was normalized to glucose-6-phosphate dehydrogenase (G6PD). For mitochondrial DNA content measurement, DNA was extracted following Hoffman's protocol, then digested with RNase (Hoffman and Winston, 1987). COX2 gene (COX2 F: GTGATGAAGTTATTTACCAGC, COX2 R: ATTCAACAGTTTCACCACTATC) was measured as mtDNA content, ACT1 (ACT1 F: CCCAGGTATTGCCGAAAGAATGC, ACT1 R: GGAAGATGGAGCCAAAGCGG) was measured for genomic DNA content.

Cell Collection, Protein Extraction and Detection

Equal numbers of cells were collected from respective cultures and stored in -80°C. Cells were lysed in 8% trichloroacetic acid (TCA) solution by bead-beating with glass beads, following the TCA precipitation method. Protein concentrations from extracts were

measured using bicinchoninic acid assay (BCA assay, Thermo Scientific). Equal amounts of samples were resolved on 4-12% bis-tris gels. Coomassie blue–stained gels were used as loading controls. The following primary antibodies were used: monoclonal FLAG M2 (Sigma), HA (12CA5, Roche), GFP (Roche), and pS6 (Cell Signaling 2211). Secondary antibodies are horseradish peroxidase–conjugated secondary antibodies (mouse and rabbit, Sigma). Standard enhanced chemiluminescence (Thermo Scientific) was used for Western blot development.

Phosphatase Treatment

The cell lysates were split into half and treated with Lambda phosphatase (NEB) at 30 °C for 30 minutes.

Detection of Phosphorylated Sch9 by NTCB Cleavage

Sch9 phosphorylation was detected using minor adjustments to previously published methods (Urban et al., 2007). Collected samples were quenched in 10% trichloroacetic acid at 4°C, and rapidly harvested by centrifugation. The pellets were stored in -80°C and lysed in 50 mM Tris (pH 7.5), 5 mM EDTA, 6 M urea, 1% SDS, 1 mM phenylmethylsulfonyl fluoride (PMSF), and protein phosphatase inhibitors (50 mM sodium fluoride, 2 mM sodium orthovanadate) with bead-beating. The lysates were heated at 65°C then centrifuged. The protein lysates were equalized according to protein concentration, then cleaved by treatment with 2 mM 2-nitro-5-thiocyanatobenzoic acid (NTCB) in 0.1 M CHES (pH 10.5) at room temperature overnight. Further analysis was done by 8% SDS–polyacrylamide gel electrophoresis and immunoblot with the HA antibody.

Phos-tag Gel Electrophoresis

Homemade phostag gel was made with Phos-Tag™ (Wako Laboratory Chemical). The gel was run at 80 V through stacking, 100 V for resolving, then washed with EDTA containing transfer buffer before transferring for 2 hours at 80 V.

Coomassie Blue Staining

SDS-PAGE gel was washed with ultrapure water then stained with SimplyBlue™ SafeStain (Thermo Fisher Scientific) for 1 hour, then washed with ultrapure water to destain.

Cells for Metabolite Extractions

Cells were grown in YPD overnight, then diluted in YPD ($OD_{600} = 0.2$) and grown to $OD_{600} \sim 1.0$. The cells were either collected for metabolite extractions or transferred to SD and then collected for metabolite extractions at specific time points. Collected cells were cold quenched in a -40°C methanol bath, spun down at 4°C , extracted with HPLC grade 75% ethanol and heated for 3 minutes at 85°C as described previously (Castrillo et al., 2003). The supernatants with metabolites were collected and dried down.

Metabolite Analysis by LC-MS/MS

Extracted metabolites were measured using targeted LC-MS/MS methods described previously (Laxman et al., 2014). The relative amounts were either compared directly among genotypes or normalized against that of WT at the first time point.

Halo Assay

Same OD of cells were spread on to freshly prepared SD plate. Autoclaved Whatman Filter Paper (Sigma-Aldrich) was soaked in 1M H_2O_2 , drained for excessive liquid, then put into on the middle of the agar. The plate is incubated for 2 days at 30°C .

¹⁵N-Ammonium Sulfate or ¹³C-Glucose or Labeling and Tracer Analysis

Cells were grown in YPD to OD₆₀₀ ~ 1.0 and switched to SD at OD₆₀₀ = 0.2 and grown to OD₆₀₀ ~ 0.5. Then cells were collected for metabolite extraction or switched to SD where all the ammonium sulfate was ¹⁵N-labeled ammonium sulfate [(¹⁵NH₄)₂SO₄] (Cambridge Isotope Laboratories Inc) or all glucose was ¹³C-glucose (Sigma-Aldrich). ¹⁵N-labeled or ¹³C-labeled metabolites were extracted at indicated times and detected by LC-MS/MS, with the targeted parent and daughter ions specific to the ¹⁵N or ¹³C forms of the metabolites.

¹³C-Acetate Labeling and Tracer Analysis

Cells were grown in YPD to OD₆₀₀ ~ 1.0 and switched to SD at OD₆₀₀ = 0.2 and grown to OD₆₀₀ ~ 0.5. Then 2 mM ¹³C₂-acetate was added to the medium (Sigma-Aldrich). ¹³C-labeled metabolites were extracted at indicated times and detected by LC-MS/MS, with the targeted parent and daughter ions specific to the ¹³C forms of the metabolites.

Glucose and NAD⁺/NADH Measurements

Medium was collected from different time points and spun to collect the supernatant. The glucose concentration of the medium was measured with Glucose(GO) Assay Kit (Sigma-Aldrich) at A₅₇₀, the exact values were calculated according to standard curve. NAD⁺/NADH ratios were measured as described previously (Kern et al., 2014).

Dissolved Oxygen Level Measurement

Dissolved oxygen levels during batch growth was measured with a Multifors Fermentor (Infors HT). 10 ODs of cells were inoculated into 500 mL of SD in dual fermentor vessels running side by side with the same medium. IRIS v5 software was used to record the pH and dissolved oxygen concentration.

Live Cell Imaging

Cells were grown in YPD to log phase then transferred to SD and subjected to the indicated treatments before imaging using a DeltaVision RT imaging system with a 100x oil-immersion objective. Images were deconvoluted then processed by ImageJ.

Hierarchical Clustering Analysis and Heat Maps

The normalized abundances of metabolites were \log_2 -transformed, centered about the mean, and clustered by Spearman rank correlation with the software Cluster 3.0. The data were visualized as heat maps with the software Java TreeView (created by Alok).

Bibliography

- Algret, R., Fernandez-Martinez, J., Shi, Y., Kim, S.J., Pellarin, R., Cimercanic, P., Cochet, E., Sali, A., Chait, B.T., Rout, M.P., et al. (2014). Molecular architecture and function of the SEA complex, a modulator of the TORC1 pathway. *Molecular & cellular proteomics : MCP* 13, 2855-2870.
- Bar-Peled, L., Chantranupong, L., Cherniack, A.D., Chen, W.W., Ottina, K.A., Grabiner, B.C., Spear, E.D., Carter, S.L., Meyerson, M., and Sabatini, D.M. (2013). A Tumor suppressor complex with GAP activity for the Rag GTPases that signal amino acid sufficiency to mTORC1. *Science (New York, N.Y.)* 340, 1100-1106.
- Beck, T., and Hall, M.N. (1999). The TOR signalling pathway controls nuclear localization of nutrient-regulated transcription factors. *Nature* 402, 689-692.
- Ben-Sahra, I., Howell, J.J., Asara, J.M., and Manning, B.D. (2013). Stimulation of de novo pyrimidine synthesis by growth signaling through mTOR and S6K1. *Science (New York, N.Y.)* 339, 1323-1328.
- Ben-Sahra, I., Hoxhaj, G., Ricoult, S.J., Asara, J.M., and Manning, B.D. (2016). mTORC1 induces purine synthesis through control of the mitochondrial tetrahydrofolate cycle. *Science (New York, N.Y.)* 351, 728-733.
- Bender, T., Pena, G., and Martinou, J.C. (2015). Regulation of mitochondrial pyruvate uptake by alternative pyruvate carrier complexes. *The EMBO journal* 34, 911-924.
- Binda, M., Peli-Gulli, M.P., Bonfils, G., Panchaud, N., Urban, J., Sturgill, T.W., Loewith, R., and De Virgilio, C. (2009). The Vam6 GEF controls TORC1 by activating the EGO complex. *Molecular cell* 35, 563-573.
- Birsoy, K., Wang, T., Chen, W.W., Freinkman, E., Abu-Remaileh, M., and Sabatini, D.M. (2015). An Essential Role of the Mitochondrial Electron Transport Chain in Cell Proliferation Is to Enable Aspartate Synthesis. *Cell* 162, 540-551.
- Buescher, J.M., Antoniewicz, M.R., Boros, L.G., Burgess, S.C., Brunengraber, H., Clish, C.B., DeBerardinis, R.J., Feron, O., Frezza, C., Ghesquiere, B., et al. (2015). A roadmap for interpreting (13)C metabolite labeling patterns from cells. *Current opinion in biotechnology* 34, 189-201.
- Butow, R.A., and Avadhani, N.G. (2004). Mitochondrial signaling: the retrograde response. *Molecular cell* 14, 1-15.
- Cardaci, S., Zheng, L., MacKay, G., van den Broek, N.J., MacKenzie, E.D., Nixon, C., Stevenson, D., Tumanov, S., Bulusu, V., Kamphorst, J.J., et al. (2015). Pyruvate carboxylation enables growth of SDH-deficient cells by supporting aspartate biosynthesis. *Nature cell biology* 17, 1317-1326.

Cardenas, M.E., Cutler, N.S., Lorenz, M.C., Di Como, C.J., and Heitman, J. (1999). The TOR signaling cascade regulates gene expression in response to nutrients. *Genes & development* 13, 3271-3279.

Castrillo, J.I., Hayes, A., Mohammed, S., Gaskell, S.J., and Oliver, S.G. (2003). An optimized protocol for metabolome analysis in yeast using direct infusion electrospray mass spectrometry. *Phytochemistry* 62, 929-937.

Cooper, T.G. (2002). Transmitting the signal of excess nitrogen in *Saccharomyces cerevisiae* from the Tor proteins to the GATA factors: connecting the dots. *FEMS microbiology reviews* 26, 223-238.

Costanzo, M., Baryshnikova, A., Bellay, J., Kim, Y., Spear, E.D., Sevier, C.S., Ding, H., Koh, J.L., Toufighi, K., Mostafavi, S., et al. (2010). The genetic landscape of a cell. *Science (New York, N.Y.)* 327, 425-431.

Courchesne, W.E., and Magasanik, B. (1988). Regulation of nitrogen assimilation in *Saccharomyces cerevisiae*: roles of the URE2 and GLN3 genes. *Journal of bacteriology* 170, 708-713.

Crespo, J.L., Powers, T., Fowler, B., and Hall, M.N. (2002). The TOR-controlled transcription activators GLN3, RTG1, and RTG3 are regulated in response to intracellular levels of glutamine. *Proceedings of the National Academy of Sciences of the United States of America* 99, 6784-6789.

Diaz-Troya, S., Perez-Perez, M.E., Florencio, F.J., and Crespo, J.L. (2008). The role of TOR in autophagy regulation from yeast to plants and mammals. *Autophagy* 4, 851-865.

Dokudovskaya, S., Waharte, F., Schlessinger, A., Pieper, U., Devos, D.P., Cristea, I.M., Williams, R., Salamero, J., Chait, B.T., Sali, A., et al. (2011). A conserved coatmer-related complex containing Sec13 and Seh1 dynamically associates with the vacuole in *Saccharomyces cerevisiae*. *Molecular & cellular proteomics : MCP* 10, M110.006478.

Duran, R.V., Oppliger, W., Robitaille, A.M., Heiserich, L., Skendaj, R., Gottlieb, E., and Hall, M.N. (2012). Glutaminolysis activates Rag-mTORC1 signaling. *Molecular cell* 47, 349-358.

Elbaz-Alon, Y., Rosenfeld-Gur, E., Shinder, V., Futerman, A.H., Geiger, T., and Schuldiner, M. (2014). A dynamic interface between vacuoles and mitochondria in yeast. *Developmental cell* 30, 95-102.

Fabrizio, P., Pozza, F., Pletcher, S.D., Gendron, C.M., and Longo, V.D. (2001). Regulation of longevity and stress resistance by Sch9 in yeast. *Science (New York, N.Y.)* 292, 288-290.

- Godard, P., Urrestarazu, A., Vissers, S., Kontos, K., Bontempi, G., van Helden, J., and Andre, B. (2007). Effect of 21 different nitrogen sources on global gene expression in the yeast *Saccharomyces cerevisiae*. *Molecular and cellular biology* 27, 3065-3086.
- Gonzalez, A., Shimobayashi, M., Eisenberg, T., Merle, D.A., Pendl, T., Hall, M.N., and Moustafa, T. (2015). TORC1 promotes phosphorylation of ribosomal protein S6 via the AGC kinase Ypk3 in *Saccharomyces cerevisiae*. *PloS one* 10, e0120250.
- Heitman, J., Movva, N.R., and Hall, M.N. (1991). Targets for cell cycle arrest by the immunosuppressant rapamycin in yeast. *Science (New York, N.Y.)* 253, 905-909.
- Hoffman, C.S., and Winston, F. (1987). A ten-minute DNA preparation from yeast efficiently releases autonomous plasmids for transformation of *Escherichia coli*. *Gene* 57, 267-272.
- Huber, A., French, S.L., Tekotte, H., Yerlikaya, S., Stahl, M., Perepelkina, M.P., Tyers, M., Rougemont, J., Beyer, A.L., and Loewith, R. (2011). Sch9 regulates ribosome biogenesis via Stb3, Dot6 and Tod6 and the histone deacetylase complex RPD3L. *The EMBO journal* 30, 3052-3064.
- Jauert, P.A., Jensen, L.E., and Kirkpatrick, D.T. (2005). A novel yeast genomic DNA library on a geneticin-resistance vector. *Yeast (Chichester, England)* 22, 653-657.
- Jewell, J.L., Kim, Y.C., Russell, R.C., Yu, F.X., Park, H.W., Plouffe, S.W., Tagliabracci, V.S., and Guan, K.L. (2015). Metabolism. Differential regulation of mTORC1 by leucine and glutamine. *Science (New York, N.Y.)* 347, 194-198.
- Kaeberlein, M., Powers, R.W., 3rd, Steffen, K.K., Westman, E.A., Hu, D., Dang, N., Kerr, E.O., Kirkland, K.T., Fields, S., and Kennedy, B.K. (2005). Regulation of yeast replicative life span by TOR and Sch9 in response to nutrients. *Science (New York, N.Y.)* 310, 1193-1196.
- Kalderon, D., Roberts, B.L., Richardson, W.D., and Smith, A.E. (1984). A short amino acid sequence able to specify nuclear location. *Cell* 39, 499-509.
- Kamada, Y., Yoshino, K., Kondo, C., Kawamata, T., Oshiro, N., Yonezawa, K., and Ohsumi, Y. (2010). Tor directly controls the Atg1 kinase complex to regulate autophagy. *Molecular and cellular biology* 30, 1049-1058.
- Kayikci, O., and Nielsen, J. (2015). Glucose repression in *Saccharomyces cerevisiae*. *FEMS yeast research* 15.

Kern, S.E., Price-Whelan, A., and Newman, D.K. (2014). Extraction and measurement of NAD(P)(+) and NAD(P)H. *Methods in molecular biology* (Clifton, N.J.) *1149*, 311-323.

Kim, E., Goraksha-Hicks, P., Li, L., Neufeld, T.P., and Guan, K.L. (2008). Regulation of TORC1 by Rag GTPases in nutrient response. *Nature cell biology* *10*, 935-945.

Komeili, A., Wedaman, K.P., O'Shea, E.K., and Powers, T. (2000). Mechanism of metabolic control. Target of rapamycin signaling links nitrogen quality to the activity of the Rtg1 and Rtg3 transcription factors. *The Journal of cell biology* *151*, 863-878.

Koning, A.J., Lum, P.Y., Williams, J.M., and Wright, R. (1993). DiOC6 staining reveals organelle structure and dynamics in living yeast cells. *Cell motility and the cytoskeleton* *25*, 111-128.

Korshunov, S.S., Skulachev, V.P., and Starkov, A.A. (1997). High protonic potential actuates a mechanism of production of reactive oxygen species in mitochondria. *FEBS letters* *416*, 15-18.

Kuang, Z., Cai, L., Zhang, X., Ji, H., Tu, B.P., and Boeke, J.D. (2014). High-temporal-resolution view of transcription and chromatin states across distinct metabolic states in budding yeast. *Nature structural & molecular biology* *21*, 854-863.

Laxman, S., Sutter, B.M., Shi, L., and Tu, B.P. (2014). Npr2 inhibits TORC1 to prevent inappropriate utilization of glutamine for biosynthesis of nitrogen-containing metabolites. *Science signaling* *7*, ra120.

Liao, X., and Butow, R.A. (1993). RTG1 and RTG2: two yeast genes required for a novel path of communication from mitochondria to the nucleus. *Cell* *72*, 61-71.

Liu, Z., and Butow, R.A. (1999). A transcriptional switch in the expression of yeast tricarboxylic acid cycle genes in response to a reduction or loss of respiratory function. *Molecular and cellular biology* *19*, 6720-6728.

Loewith, R., and Hall, M.N. (2011). Target of rapamycin (TOR) in nutrient signaling and growth control. *Genetics* *189*, 1177-1201.

Loewith, R., Jacinto, E., Wullschleger, S., Lorberg, A., Crespo, J.L., Bonenfant, D., Oppliger, W., Jenoe, P., and Hall, M.N. (2002). Two TOR complexes, only one of which is rapamycin sensitive, have distinct roles in cell growth control. *Molecular cell* *10*, 457-468.

Longtine, M.S., McKenzie, A., 3rd, Demarini, D.J., Shah, N.G., Wach, A., Brachat, A., Philippsen, P., and Pringle, J.R. (1998). Additional modules for versatile and economical PCR-based gene deletion and modification in *Saccharomyces cerevisiae*. *Yeast* (Chichester, England) *14*, 953-961.

MacGurn, J.A., Hsu, P.C., Smolka, M.B., and Emr, S.D. (2011). TORC1 regulates endocytosis via Npr1-mediated phosphoinhibition of a ubiquitin ligase adaptor. *Cell* *147*, 1104-1117.

Magasanik, B., and Kaiser, C.A. (2002). Nitrogen regulation in *Saccharomyces cerevisiae*. *Gene* *290*, 1-18.

Merhi, A., and Andre, B. (2012). Internal amino acids promote Gap1 permease ubiquitylation via TORC1/Npr1/14-3-3-dependent control of the Bul arrestin-like adaptors. *Molecular and cellular biology* *32*, 4510-4522.

Nakashima, A., Maruki, Y., Imamura, Y., Kondo, C., Kawamata, T., Kawanishi, I., Takata, H., Matsuura, A., Lee, K.S., Kikkawa, U., et al. (2008). The yeast Tor signaling pathway is involved in G2/M transition via polo-kinase. *PloS one* *3*, e2223.

Nakashima, N., Noguchi, E., and Nishimoto, T. (1999). *Saccharomyces cerevisiae* putative G protein, Gtr1p, which forms complexes with itself and a novel protein designated as Gtr2p, negatively regulates the Ran/Gsp1p G protein cycle through Gtr2p. *Genetics* *152*, 853-867.

Neklesa, T.K., and Davis, R.W. (2009). A genome-wide screen for regulators of TORC1 in response to amino acid starvation reveals a conserved Npr2/3 complex. *PLoS genetics* *5*, e1000515.

Nicklin, P., Bergman, P., Zhang, B., Triantafellow, E., Wang, H., Nyfeler, B., Yang, H., Hild, M., Kung, C., Wilson, C., et al. (2009). Bidirectional transport of amino acids regulates mTOR and autophagy. *Cell* *136*, 521-534.

Panchaud, N., Peli-Gulli, M.P., and De Virgilio, C. (2013). Amino acid deprivation inhibits TORC1 through a GTPase-activating protein complex for the Rag family GTPase Gtr1. *Science signaling* *6*, ra42.

Perry, S.W., Norman, J.P., Barbieri, J., Brown, E.B., and Gelbard, H.A. (2011). Mitochondrial membrane potential probes and the proton gradient: a practical usage guide. *BioTechniques* *50*, 98-115.

Rai, R., Tate, J.J., Shanmuganatham, K., Howe, M.M., Nelson, D., and Cooper, T.G. (2015). Nuclear Gln3 Import Is Regulated by Nitrogen Catabolite Repression Whereas Export Is Specifically Regulated by Glutamine. *Genetics* *201*, 989-1016.

Reinke, A., Anderson, S., McCaffery, J.M., Yates, J., 3rd, Aronova, S., Chu, S., Fairclough, S., Iverson, C., Wedaman, K.P., and Powers, T. (2004). TOR complex 1 includes a novel component, Tco89p (YPL180w), and cooperates with Ssd1p to maintain cellular integrity in *Saccharomyces cerevisiae*. *The Journal of biological chemistry* *279*, 14752-14762.

- Rousselet, G., Simon, M., Ripoche, P., and Buhler, J.M. (1995). A second nitrogen permease regulator in *Saccharomyces cerevisiae*. *FEBS letters* 359, 215-219.
- Rubin, A.L. (1990). Suppression of transformation by and growth adaptation to low concentrations of glutamine in NIH-3T3 cells. *Cancer research* 50, 2832-2839.
- Sancak, Y., Bar-Peled, L., Zoncu, R., Markhard, A.L., Nada, S., and Sabatini, D.M. (2010). Ragulator-Rag complex targets mTORC1 to the lysosomal surface and is necessary for its activation by amino acids. *Cell* 141, 290-303.
- Schmidt, A., Beck, T., Koller, A., Kunz, J., and Hall, M.N. (1998). The TOR nutrient signalling pathway phosphorylates NPR1 and inhibits turnover of the tryptophan permease. *The EMBO journal* 17, 6924-6931.
- Sekito, T., Liu, Z., Thornton, J., and Butow, R.A. (2002). RTG-dependent mitochondria-to-nucleus signaling is regulated by MKS1 and is linked to formation of yeast prion [URE3]. *Molecular biology of the cell* 13, 795-804.
- Siniossoglou, S., Wimmer, C., Rieger, M., Doye, V., Tekotte, H., Weise, C., Emig, S., Segref, A., and Hurt, E.C. (1996). A novel complex of nucleoporins, which includes Sec13p and a Sec13p homolog, is essential for normal nuclear pores. *Cell* 84, 265-275.
- Small, W.C., Brodeur, R.D., Sandor, A., Fedorova, N., Li, G., Butow, R.A., and Srere, P.A. (1995). Enzymatic and metabolic studies on retrograde regulation mutants of yeast. *Biochemistry* 34, 5569-5576.
- Smolina, V.S., and Bekker, M.L. (1982). [Properties of 5-phosphoryl-1-pyrophosphate amidotransferase from the yeast *Saccharomyces cerevisiae* wild type and mutant with altered purine biosynthesis regulation]. *Biokhimiia (Moscow, Russia)* 47, 162-167.
- Spielewoy, N., Guaderrama, M., Wohlschlegel, J.A., Ashe, M., Yates, J.R., 3rd, and Wittenberg, C. (2010). Npr2, yeast homolog of the human tumor suppressor NPRL2, is a target of Grr1 required for adaptation to growth on diverse nitrogen sources. *Eukaryotic cell* 9, 592-601.
- Stracka, D., Jozefczuk, S., Rudroff, F., Sauer, U., and Hall, M.N. (2014). Nitrogen source activates TOR (target of rapamycin) complex 1 via glutamine and independently of Gtr/Rag proteins. *The Journal of biological chemistry* 289, 25010-25020.
- Stumvoll, M., Perriello, G., Meyer, C., and Gerich, J. (1999). Role of glutamine in human carbohydrate metabolism in kidney and other tissues. *Kidney international* 55, 778-792.
- Sugiura, Y., Katsumata, Y., Sano, M., Honda, K., Kajimura, M., Fukuda, K., and Suematsu, M. (2016). Visualization of in vivo metabolic flows reveals accelerated utilization of glucose and lactate in penumbra of ischemic heart. *Scientific reports* 6, 32361.

Sullivan, L.B., Gui, D.Y., Hosios, A.M., Bush, L.N., Freinkman, E., and Vander Heiden, M.G. (2015). Supporting Aspartate Biosynthesis Is an Essential Function of Respiration in Proliferating Cells. *Cell* *162*, 552-563.

Sutter, B.M., Wu, X., Laxman, S., and Tu, B.P. (2013). Methionine inhibits autophagy and promotes growth by inducing the SAM-responsive methylation of PP2A. *Cell* *154*, 403-415.

Thomas, G., and Hall, M.N. (1997). TOR signalling and control of cell growth. *Current opinion in cell biology* *9*, 782-787.

Trumbly, R.J. (1992). Glucose repression in the yeast *Saccharomyces cerevisiae*. *Molecular microbiology* *6*, 15-21.

Tu, B.P., Kudlicki, A., Rowicka, M., and McKnight, S.L. (2005). Logic of the yeast metabolic cycle: temporal compartmentalization of cellular processes. *Science (New York, N.Y.)* *310*, 1152-1158.

Urban, J., Soulard, A., Huber, A., Lippman, S., Mukhopadhyay, D., Deloche, O., Wanke, V., Anrather, D., Ammerer, G., Riezman, H., et al. (2007). Sch9 is a major target of TORC1 in *Saccharomyces cerevisiae*. *Molecular cell* *26*, 663-674.

Valenzuela, L., Ballario, P., Aranda, C., Filetici, P., and Gonzalez, A. (1998). Regulation of expression of GLT1, the gene encoding glutamate synthase in *Saccharomyces cerevisiae*. *Journal of bacteriology* *180*, 3533-3540.

Vowinckel, J., Hartl, J., Butler, R., and Ralser, M. (2015). MitoLoc: A method for the simultaneous quantification of mitochondrial network morphology and membrane potential in single cells. *Mitochondrion* *24*, 77-86.

Westermann, B. (2012). Bioenergetic role of mitochondrial fusion and fission. *Biochimica et biophysica acta* *1817*, 1833-1838.

Williamson, D.H., Lund, P., and Krebs, H.A. (1967). The redox state of free nicotinamide-adenine dinucleotide in the cytoplasm and mitochondria of rat liver. *The Biochemical journal* *103*, 514-527.

Wu, X., and Tu, B.P. (2011). Selective regulation of autophagy by the Iml1-Npr2-Npr3 complex in the absence of nitrogen starvation. *Molecular biology of the cell* *22*, 4124-4133.

Yuneva, M., Zamboni, N., Oefner, P., Sachidanandam, R., and Lazebnik, Y. (2007). Deficiency in glutamine but not glucose induces MYC-dependent apoptosis in human cells. *The Journal of cell biology* *178*, 93-105.